UNITED STATES

DEPARTMENT OF THE INTERIOR

GEOLOGICAL SURVEY

TECHNICAL LETTER NASA-65

DISPERSIVE MULTISPECTRAL SCANNING: A FEASIBILITY STUDY*

by

J. Braithwaite**

November 1966

The work reported herein was conducted by the Willow Run Laboratories of the Institute of Science and Technology, University of Michigan on behalf of the U.S. Geological Survey, Branch of Theoretical Geophysics, under Contract 14-08-001

*Work performed under NASA Contract No. R-146-09-020-006

**Willow Run Laboratories of the Institute of Science and Technology, University of Michigan, Ann Arbor, Michigan

UNITED STATES
DEPARTMENT OF THE INTERIOR
GEOLOGICAL SURVEY
WASHINGTON, D.C. 20242

Technical Letter
NASA-65
November 1966

Dr. Peter C. Badgley
Chief, Natural Resources Program
Office of Space Science and Applications
Code SAR, NASA Headquarters
Washington, D.C. 20546

Dear Peter:

Transmitted herewith are 3 copies of:

TECHNICAL LETTER NASA-65

DISPERSIVE MULTISPECTRAL SCANNING: A FEASIBILITY STUDY*

by

J. Braithwaite**

Sincerely yours,

William A. Fischer
Research Coordinator
Earth Orbiter Program

*Work performed under NASA Contract No. R-146/09-020-006

**Willow Run Laboratories of the Institute of Science and Technology,
University of Michigan, Ann Arbor, Michigan

CONTENTS

FOREWORD

The work on which this report is based was conducted in the Infrared and Optical Sensor Laboratory (M. R. Holter, Head) of the Willow Run Laboratories. D. S. Lowe was the principal investigator. J. Braithwaite was the principal author. Contributions on specific aspects of the work were made as follows:

R. Emmert—data processing and electronics

P. Wierenga—agriculture

S. Clark—geology

E. Work and D. Szeles—optical design

W. Brown and A. Krause—detectors and performance

The work reported is consonant with and fulfills part of the objectives of a comparative multispectral remote sensing program of the Laboratory. The goal of the program is to develop methods of improving and extending current remote sensing capabilities by using the spectral characteristics of surface features or objects being sought. Improvements are sought in the kinds and quantity of data obtainable and in the quality, speed, and economy of the imagery-interpretation process. Previous related reports issued by the Infrared and Optical Sensor Laboratory are listed on page 53.

ABSTRACT

Optical-mechanical line scanners can be used from aircraft and satellites to obtain strip maps of the surface over which the vehicle passes. The feasibility of combining wavelength dispersing techniques with such scanning techniques has been studied. This combination makes it possible to obtain spectral and spatial information simultaneously. Appropriate data processing techniques will then permit us to interpret the spectral data to produce surface maps of various kinds, such as maps of crop type or of surface geology.

Parametric equations representing a generalized dispersive multispectral scanner are developed and discussed in the light of subsystem and component state of the art and from the point of view of prospective users such as geologists and agriculturalists.

FIGURES

TABLES

DISPERSIVE MULTISPECTRAL SCANNING; A FEASIBILITY STUDY

1
INTRODUCTION AND SUMMARY

The purpose of this study is to investigate the feasibility of using multispectral spatial scanning techniques in terrestrial and lunar orbital experiments and, more specifically, in exploratory airborne experiments which would be carried out prior to the orbiting experiments. In particular, it is to explore the feasibility and advantages of combining dispersive spectral techniques with optical-mechanical scanning techniques throughout the 0.3-25-μ wavelength range. The properties of instruments employing these techniques have been analyzed and are discussed from the point of view of geological and agricultural applications.

The detector of an optical-mechanical scanner can be replaced by a dispersing monochromator or spectrograph, but the specifications of the two parts of the combined instrument are not independent. For instance, changing the spectrograph entrance slit size will alter both the spatial scanning resolution and the spectral resolution, assuming, of course, that no other changes are made.

The most important part of this study was thought to be an investigation of the possibilities and limitations arising from the geometry of the system and the performance available from state-of-the-art components and subsystems. The derivation of the relevant parametric equations is given in the appendix. The equations are listed and their implications discussed in section 2. Although the sensitivity equations are the most important of these equations, the length of the detector array will to a large extent determine the practicability of the number of channels in a particular system. The reasons are that there are obviously practical limits to the sizes of cryostat and detector array, and that the overall size of the dispersing optics will be closely related to the array length. It should be noticed that the array length is proportional to the number of contiguous spectral channels and to the angular instaneous field of the spatial scan but not to the spectral resolution.

Little attention has been paid to those subsystems and components that are well within the state of the art. Thus, for instance, the optical and mechanical design of the spatial scanner and telescope is barely mentioned. However, discussions of several of the more critical components and subsystems are given in section 3. It becomes clear that, although the design of the

dispersing optical systems is certainly feasible, the compactness of the overall system will depend on the f-number obtained in this part of the optical design. Both the length of the dispersing optical system and the length of the detector array are proportional to this f-number. The limited optical design carried out in this feasibility study did not permit exact configuration of this part of the instrument. Detailed optical designs for specific system requirements, which are beyond the scope of this study, will be required to obtain optimum designs.

A general discussion of the data processing is given. However, it quickly becomes clear that satisfactory preprocessing (i.e., prior to recording) is only possible if good statistical data are available on the spectra which are to be recognized and rejected. It is, therefore, recommended that for the airborne system, at any rate, the raw video data be recorded intact and processed on the ground in a general-purpose computer.

In section 4 an attempt is made to reconcile the requirements of geologists interested in terrestrial and lunar geology with practical instrumentation possibilities. Consideration was given to operations at a resolution of 5 cm^{-1} over the 8-25-μ region. The problems involved in achieving this resolution over such a wide range of wavelengths turn out to be very considerable. However, 40-cm^{-1} resolution over the 8-14-μ region turns out to be within the current state of the art. On the basis of current conjecture on the nature of the moon's surface, this performance would provide most of the geological information that could be derived by such remote sensing techniques. From a 75 km lunar orbit ground resolution of 1/2 km is quite practical, and in view of the limited current knowledge on the nature of the moon's surface would apparently be quite acceptable to the geologists.

A similar exercise was carried out for earth orbit agricultural applications and is reported in section 5. The result, a spectral resolving power of 10 and a spatial resolution of 1 mrad, or about 1000 ft, from the earth orbital altitudes, is a somewhat less happy compromise primarily because a much finer spatial resolution would be perferred for some applications. The compromise on spectral range is better. The range 0.3 to 2.6 μ can be adequately covered with a silica prism and appears to contain most of wavelength bands at which spectral signatures of known interest to agriculturalists occur. It is, however, recommended that this range be supplemented by two wideband channels covering 4.5 to 5.5 μ and 10 to 12 μ, respectively. These are the optimum channels for detecting temperature differences somewhat higher than and at terrestrial ambient temperatures, respectively.

In the discussion on airborne precursory experiments and equipment (sec. 6), the conclusion is reached that for some purposes it would be desirable to use separate systems for short wavelength and long-wavelength applications and that these systems should be essentially identical to

those proposed for orbital use. On the other hand for more general use, a more complicated combined system would be preferable and such a system is proposed.

2 THE USE AND IMPLICATIONS OF THE PARAMETRIC EQUATIONS

The performance of a generalized multispectral dispersive scanner (fig. 1) may be described in terms of selected system parameters through the set of parametric equations developed in the appendix. Because of the relations which exist among various parameters, the equations are not the only ones which may be used. However, these particular parametric equations use the sets of parameters which are judged to be the most useful in the sense that any one parameter in any equation can be varied, at any rate, over some range of feasible values without necessitating changes in any of the other members of the selected set.

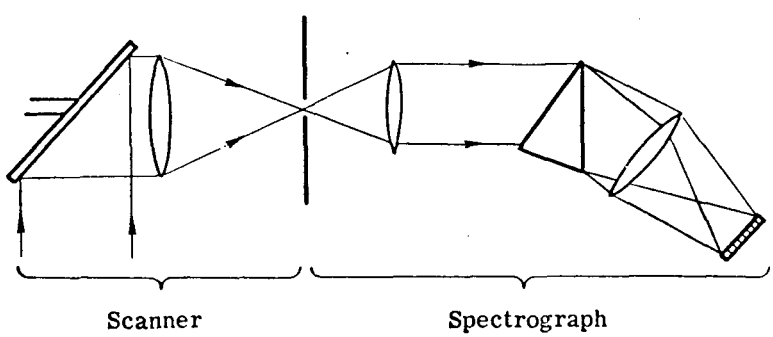

FIGURE 1. GENERALIZED OPTICAL SYSTEM

The S/N equations developed in the appendix may be used to calculate the sensitivity of a proposed system. This can be done either in terms of S/N for a given N_λ or ΔN_λ or by finding the ΔN_λ which will give the S/N needed to allow a required detection probability. Then if the performance turns out to be inadequate it is possible by inspection of the equations to find changes in the original parameters which will provide the necessary increase in performance.

For easy reference, the most important of the relations developed in the appendix are given below; they are followed by an explanation of the symbols.

$$\dot{\alpha} = \frac{2\pi(V/H)}{n\beta} \tag{2a}$$

$$\tau = \frac{n\beta^2}{2\pi(V/H)} \tag{3a}$$

$$\delta\lambda = \frac{D_1\beta}{D_2(d\theta/d\lambda)} \tag{5}$$

$$d_2 = \beta D_1 F_2 \tag{6}$$

$$d'' = m\beta D_1 F_d \tag{6b}$$

$$L = M\beta D_1 F_2 \tag{7}$$

$$\Delta f = \frac{\pi(V/H)}{\beta^2 n} \tag{11}$$

$$\left(\frac{S}{N}\right)_{I\lambda} = \frac{N_\lambda \delta\lambda'}{4}\sqrt{\frac{\pi n}{m^p}}\frac{D_1 D^* \beta^2}{F_d\sqrt{V/H}}(\text{o.e.} \times \text{s.e.}) \tag{12}$$

$$\left(\frac{S}{N}\right)_{S\lambda} = 4.2 \times 10^8 D_1\beta^2 \Delta\rho_\lambda \sqrt{\frac{nR_c H_\lambda \delta\lambda\ (\text{o.e.})}{\rho_\lambda(V/H)}} \quad (\text{s.e.}) \tag{16}$$

D_1 = scanner telescope aperture

D_2 = aperture of dispersing element

D^* = specific detectivity of solid-state detectors

d'' = width of one detector

d_2 = width of exit slit

$d\theta/d\lambda$ = angular dispersion of dispersing element

F_2 = f-number of spectrograph telescope

F_d = f-number of beam at the detector

H = vehicle altitude

H_λ = irradiance at target

M = number of spectral channels

m = $\delta\lambda'/\delta\lambda$

N_λ = target radiance

n = number of faces of scan mirror assembly

o.e. = optical efficiency

p = 2 if field lenses are used but 1 if they are not

R_c = cathode radiant sensitivity of photoemissive detector

$(S/N)_{I\lambda}$ = spectral signal-to-noise ratio when noise level is independent of signal level

$(S/N)_{S\lambda}$ = spectral signal-to-noise when signal-dependent shot noise predominates

s.e. = signal efficiency

V = vehicle velocity

$\dot{\alpha}$ = rotational speed of scan

β = instantaneous angular field of view of scanner

Δf = electronic noise bandwidth

$\Delta\rho_\lambda$ = reflectance variation

$\delta\lambda$ = instrument-limited resolved wavelength interval

$\delta\lambda'$ = resolved wavelength interval used

λ = wavelength

ρ_λ = target spectral reflectance (generally a function of angle of view and angle of illumination)

τ = dwell time

For instance, suppose that our first selection of parameters for use in equation 12 led to an S/N of 0.5, whereas 5 is needed to give adequate detection probability. Further suppose we have used the best practical values for n, m, D^*, and F, and operational considerations fix V/H and ΔN_λ. Then it is clear that the product of the remaining parameters $\delta\lambda D_1\beta^2$ must be increased by a factor of 10 or the experiment abandoned as impracticable.

It must be noticed, however, that, in any selection of the parameters occurring in the S/N equations, values for other parameters such as the detector and prism or grating sizes are implied. Thus at all times care must be taken to ensure that impractical values of parameters are neither used nor implied in the S/N equations. The remainder of this section deals with these limitations. The symbols discussed are defined above.

n. The effects of the dead time (during which parts of more than one scan mirror face cover the entrance aperture) will cause the size of the overall scan mirror assembly to increase faster than n. Also, as S/N varies with D but only with the square root of n, it may be more practical to increase D. Alternatively, it may be more practical to obtain an effective increase in n by using multiple synchronized units, of which the double-ended scanners are examples.

m. This is at best a poor way of increasing sensitivity and is best thought of as a factor to introduce the effects of increasing the effective bandwidth given by a particular spectrograph at various wavelengths.

D_1. Notice that, if D_1 is changed but all other parameters are left unchanged, then the whole instrument will scale in size in proportion to D_1.

F. Theoretically the minimum possible value of F is 1/2, and the smallest practical value will be somewhat greater, say between 0.7 and 1.0. However, it should be noticed that for radiation-noise-limited detectors in which the f-number is increased by means of a cooled shield, D^* will increase to offset the change in F.

d''. Semiconductor detectors can be made in sizes ranging from about 5 mm down to about 0.05 mm. The smaller sizes are obtained by the use of cooled apertures in front of larger detector flakes which, as a result, may have higher impedances than can be properly matched to the amplifier chain, resulting in lowered effective D^*. The dark currents of photomultipliers are negligible for our purposes, so that the photocathode area does not appear in the equations and very small photocathode areas are not required. The largest photocathode areas are about 1 sq. in., which is adequate for our purposes.

$\dot{\alpha}$. The rotational rate of the scan mirror must not exceed appropriate engineering limits. However, because for both earth and lunar orbits $V/H \sim 0.025$ and β is of the order of 10^{-3} rad, a typical value for $\dot{\alpha}$ is 1500 rpm, which is quite practical.

τ. The dwell time should not be less than the detector and associated electronic time constant, or the effective value of D^* will fall off. Again with $\beta^2 \sim 10^{-6}$ and $V/H \sim 0.025$, we find $\tau \sim 6$ μsec. Thus most detectors likely to be used have adequate time constants provided they are used correctly. Exceptions are some of the film-type detectors such as those made with lead sulfide.

$\delta\lambda$ and D_2. Equation 5 relates these to the prism or grating dispersion and the scanner parameters D and β. This relation can be thought of as a way to determine the size of dispersing element (D_2) needed if a particular prism material or grating spacing is used. As will be seen in section 3.1, it quickly becomes apparent that prisms are not practical for long wavelengths or large β.

Detector array length is given by equation 7. This is perhaps one of the most important equations because, if the array is more than a few inches long, the optical system and, for cooled detectors, the cryogenic system, become very large and complicated. Thus in practice M, the number of spectral channels, is likely to be limited. For example, for the set of values of β and D recommended in sec. 4 for lunar orbital experiments and for $F_2 = 2.5$, we find

$$\text{Array length} = M/4 \text{ cm}$$

Thus even for 20 optimum spectral intervals the array length is 5 cm, or 2 in. Note that M, the number of spectral intervals, and not the spectral resolution or the spectral range individually is limited. However, these too will have restrictions imposed by other practical limitations such as the limited wavelength range over which any grating or prism material can be used efficiently.

3
SUBSYSTEMS AND COMPONENTS

3.1. OPTICAL SYSTEMS

The properties of a typical multispectral scanner are discussed in section 2 with the system of the schematic diagram of figure 1 as a basis for the discussion. An arrangement very similar to this is now being built by WRL and is soon to be flown (see fig. 2). This configuration is intended for operation in the 0.4-1.0-μ spectral region, and it is necessarily limited to this region by the spectral transmission of the high-speed, multielement camera lenses (the availability of which make the system possible) and of the optical fibers.

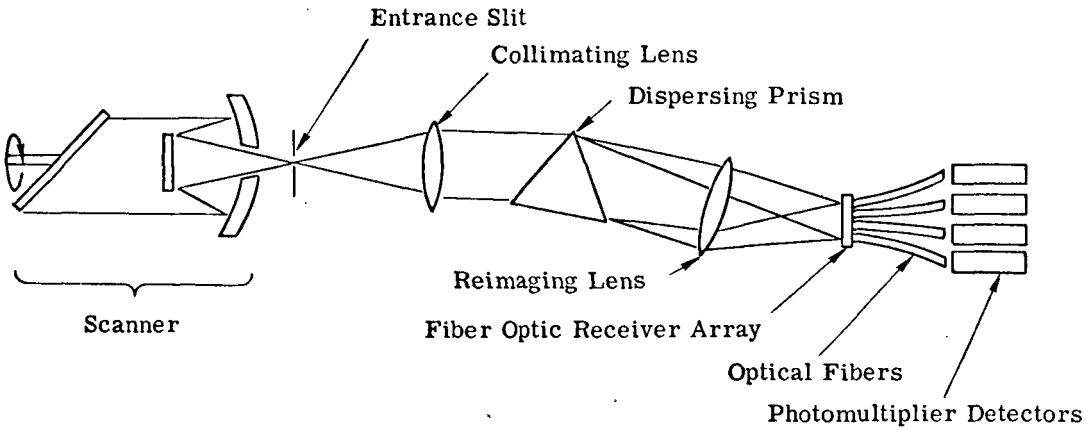

FIGURE 2. EXISTING DISPERSIVE MULTISPECTRAL SCANNER

A problem which is inherent in the design of a spatial scanner-spectrometer detector system is illustrated by the system shown in figure 2. The single detector of a conventional spectrometer or monochromator observes one spectral resolution element at any one time, and the system scans in time through the spectral region of interest. However, orbital scanners of the kind in which we are interested scan across one ground resolution element in times which are short compared with the scan time for the fastest scanning spectrometers. Therefore, the system must be designed to detect all spectral resolution bands simultaneously and must use multiple detectors. This simultaneous spectral observation by an array of detectors imposes several rather severe requirements on the spectrometer optics. The same spectral dispersing element (the prism in fig. 2) must be capable of operating over the entire spectral range of interest. It is also most desirable that its spectral dispersion ($d\theta/d\lambda$) be reasonably matched to the resolution desired throughout the region of operation.

Both reflecting and refractive spectrographs have been used for many years in laboratories and in industry, mainly in the photographic region; and they use photographic plates as detectors. These are either concave grating instruments working at very large f-numbers of transmission prism instruments using simple lens collimators and telescopes, again using large f-numbers. Although such instruments could be matched to a scanner they would be cumbersome; and spectrographs with reasonable f-numbers of, say, 4 or 5 or even faster would be preferable. Because appreciably lower spectral resolution is required, much faster systems should indeed be possible.

A detailed optical design study is outside the scope of this study; however, the WRL optical design computing facilities were used to determine the feasibility of spectrographs working at approximately f/4. A refracting system using a single-element autocollimating lens and a Fastie-Ebert type of reflecting system were considered as examples of refracting and reflecting systems most likely to give adequate results. Equivalent specifications were imposed on both systems so that the results would be directly comparable. The 8-25-μ region was arbitrarily chosen for the analysis, and potassium bromide used as the best lens material for this wavelength region. The analysis was restricted to the use of spherical surfaces because it was hoped that aspheric surfaces would prove unnecessary.

Figures 3 and 4 are scale drawings of the two systems showing pertinent dimensions.* The dimensions given in these drawings constitute the input data which was used in performing an optical-design and a ray-trace analysis of the two systems. Rays of radiation having wavelengths of 8.0, 12.5, 16.5, and 25.0 μ are traced through both systems. The 8.0- and 25.0-μ rays were chosen because of their being at the extreme ends of the spectrum under consideration, the 12.5-μ ray because it is the first-order harmonic of 25.0-μ, and the 16.5-μ ray simply because it fills a gap and provides an additional design point.

Optimization and analysis of the two systems were carried out on an IBM 7090 computer using a WRL optical design program. This program utilizes a least square technique of the distribution of ray deviations in the image plane to determine the figure of merit for the optical system. Design parameters are then changed to reduce the figure of merit. This procedure is repeated until the desired state of optical correction is reached or the merit function cannot be reduced further. The resultant designs were evaluated by printouts of spot diagrams and a statistical analysis of these spot diagrams.

*If prisms rather than gratings are used the beams reaching and leaving the prism are on opposite sides of the prism, as shown in figures 4 and 16. This simplifies the layout slightly but does not affect the optical design.

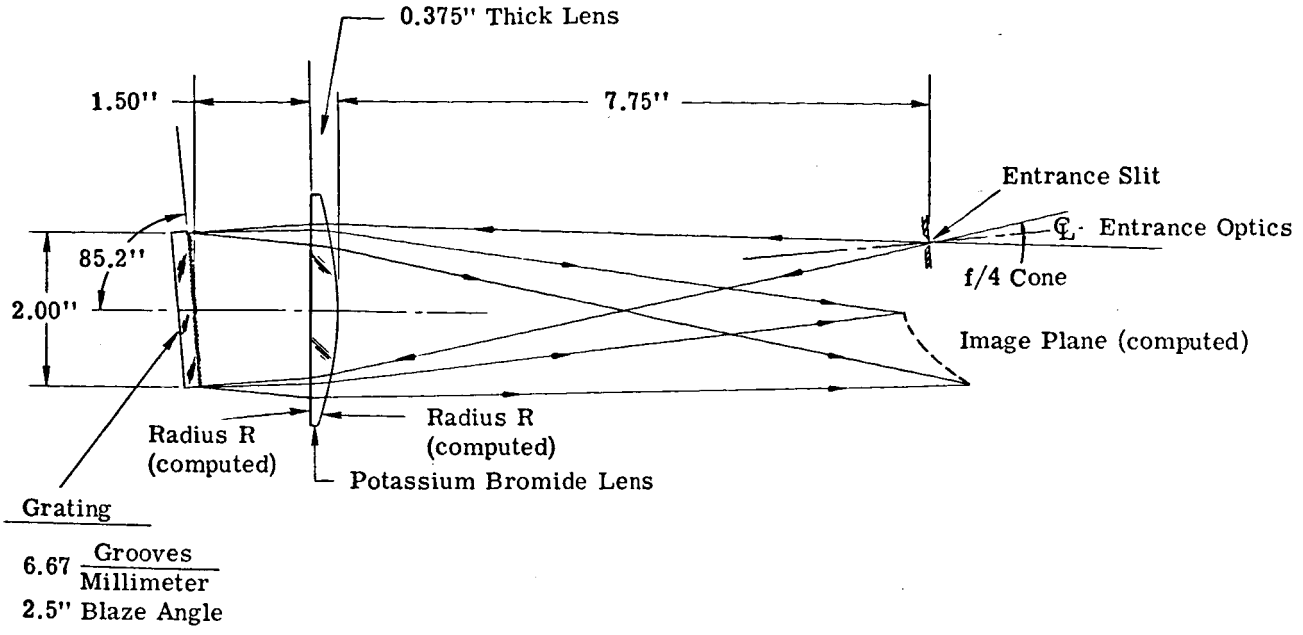

FIGURE 3. REFRACTIVE SPECTROGRAPH

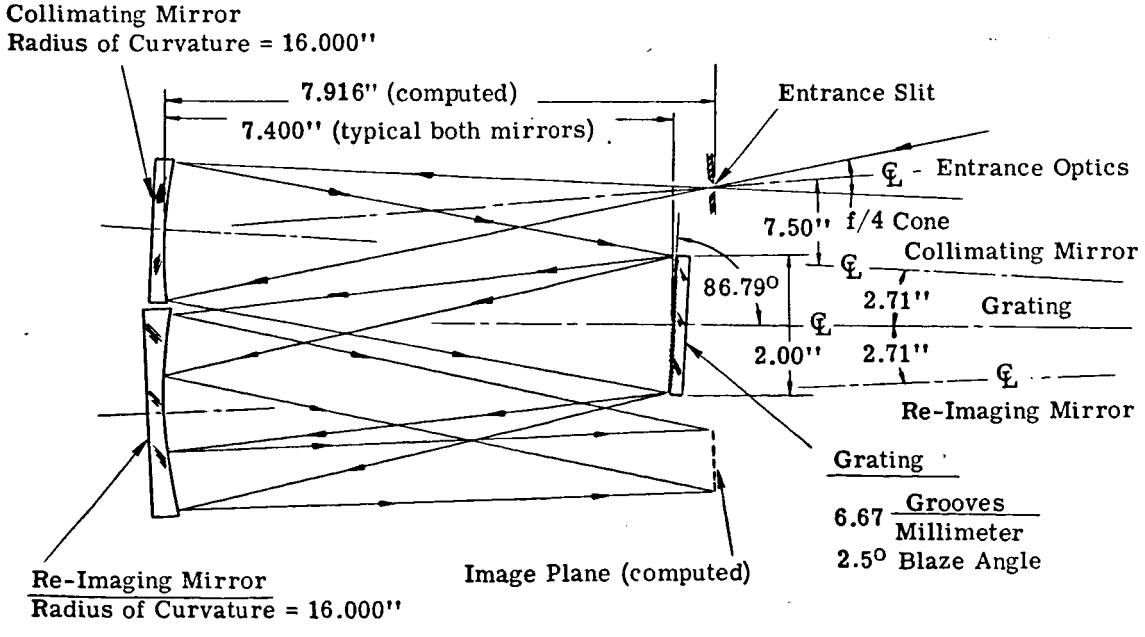

FIGURE 4. CZERNY-TURNER SPECTROGRAPH

Table I presents the computed optical characteristics for the wavelengths at which ray traces were made for a 7-channel spectrometer. Figure 5 shows scaled diagrams of the size and shape of the image plane and the relative size of the several blur circles. The elliptically shaped figures of the blur diagrams represent the enclosures encompassing 100% of the distributed energy.

TABLE I. COMPUTED OPTICAL CHARACTERISTICS

Refractive System
- Radius of curvature, lens surface R_1: 4.8196"
- Radius of curvature, lens surface R_2: 25.6947"
- Blur circle diameters (concentric to chief ray)
  - For 8.0 μ: 0.130" diameter
  - 12.5 μ: 0.118" diameter
  - 16.5 μ: 0.108" diameter
  - 25.0 μ: 0.096" diameter

Czerny-Turner System
- Distance entract slit to collimating mirror: 7.916"
- Blur circle diameters (concentric to chief ray)
  - For 8.0 μ: 0.034" diameter
  - 12.5 μ: 0.036" diameter
  - 16.5 μ: 0.038" diameter
  - 25.0 μ: 0.054" diameter

Note: Either system when combined with a scanner having a 6-in. aperture and a 0.0066-rad instantaneous field will have an optimum detector dimension of 0.16-in., as shown by the dashed squares in figure 5.

The results of the optical analysis indicate that the aberrations of the refracting system would be just acceptable but that the highly inclined focal plane would present problems for a detector array. On the other hand the performance of the reflective system is much superior on both counts. In both cases, the symmetry of the blur circles suggests that spherical aberration is a bigger limitation than coma or astigmatism, so that the use of aspheric surfaces might give considerable improvment and allow the use of appreciably faster systems. It must be remembered, however, that the length of the detector array required depends on the number of resolved channels and on the scanner's instantaneous field, among other things, so that these parameters must have a considerable bearing on the optical design of the dispersing system.

To summarize: it is clear that spectrograph-type optics can be matched to any scanner, but the compactness of the system and the number of feasible channels can be determined only through a detailed optical design for the specific system.

Dispersion Techniques. In principle, the dispersion of a prism can be controlled by varying the apex angle and by using multipass techniques. For a grating, dispersion is controlled by

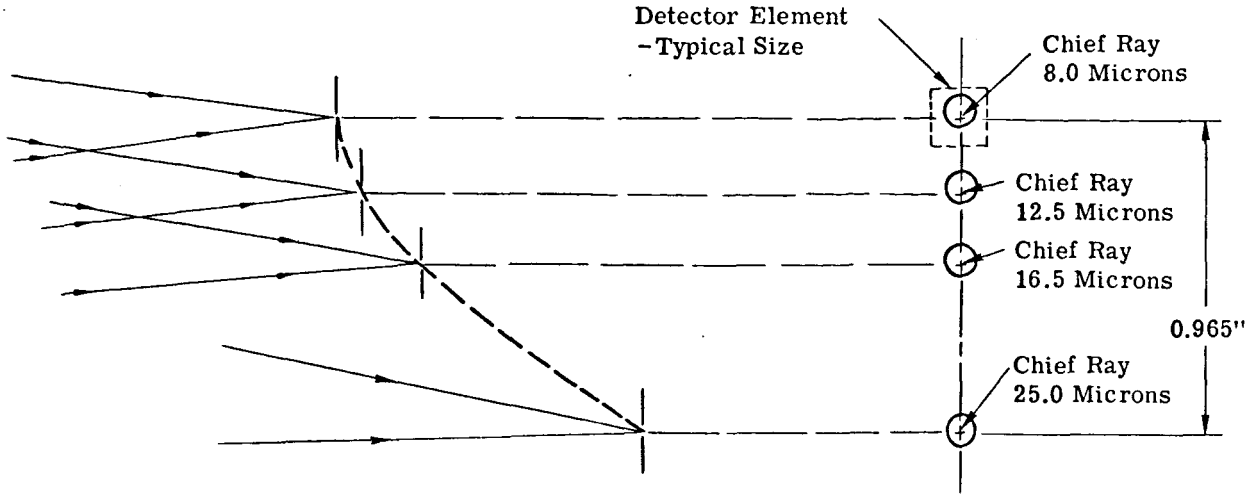

Image Plane Profile
Incidence of Chief Rays for Selected Wavelengths is Shown

Projected View-Image Plane
Image Blur for Selected Wavelengths is Indicated

(a) Double-Pass Refractive System

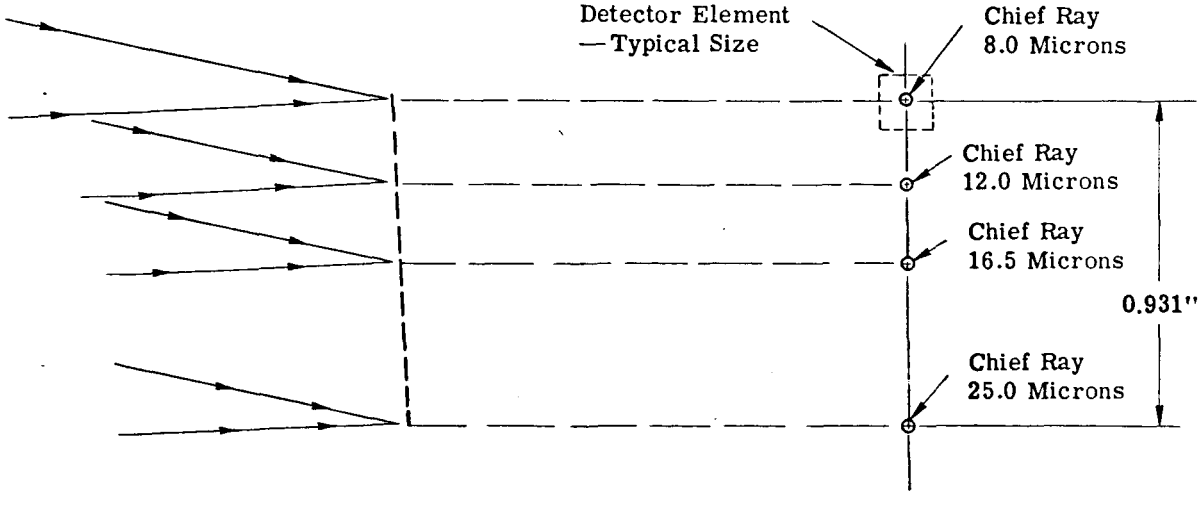

Image Plane—Profile
Incidence of Chief Rays for Selected Wavelengths is Shown

Projected View—Image Plane
Image Blur for Selected Wavelengths is Indicated

(b) Czerny-Turner System

FIGURE 5. IMAGING CHARACTERISTICS

varying the line spacing. It is not practical, however, to use an apex angle greater than about 60^{o}, nor is it possible to use a grating at wavelengths greater than the line spacing. It is also clear that, although a 60^{o} prism might be double passed by means of a Littrow mirror, multiple passing of a spectrograph collimator will seriously limit the spectral range of the instrument as a result of the difficulty of keeping the divergent resolved beams inside the apertures of the system.

The limitations of dispersing mediums are illustrated in figure 6. On this figure, the spectral intervals predicted by use of equation 5 for a variety of prism materials and of grating line spacings are given as a function of wavelength. It must be remembered that this example refers directly to a system with the following specifications only:

(1) Angular field of view, β: 0.0067 rad
(2) Collector diameter, D_1: 15 cm
(3) Prism or grating aperture, D_2: 5 cm
(4) Prism apex angle = 60^{o}

However, it is a simple matter to obtain corresponding results for other systems by use of the relation

$$\delta\lambda \propto D_1\beta/D_2$$

to change the vertical scale as appropriate. In the example chosen it will be seen that the resolving power, $R = d\lambda/\lambda$ is less than unity over wide ranges of wavelengths for all the prism materials except dense flint. However, if the field angle β can be reduced to 1 mrad and a 10-cm prism can be used, then it will be seen that resolving powers of 10 are readily obtained.

It will also be seen that gratings give uniform wavelength resolution, (in practice this is only approximately true because of angular effects) whereas that of prisms varies considerably with wavelength. Resolving power can always be reduced at a given wavelength by the use of larger detectors; but as explained in the appendix this degrades the sensitivity of the system.

It should also be remembered that the efficiency of a currently blazed grating falls off rapidly outside about a 1-octave wavelength range, through with careful design and the acceptance of some losses at the extreme wavelengths a range of 1 to 3 in wavelength can be covered.

The use of some form of image slicer to convert the square field stop of the scanner to a slit-shaped entrance for the spectrograph should be considered because the overall size of the spectrograph could then be reduced. However, as this does not seem to be essential and as image slicers are generally inefficient and quite bulky, this idea has not been followed further.

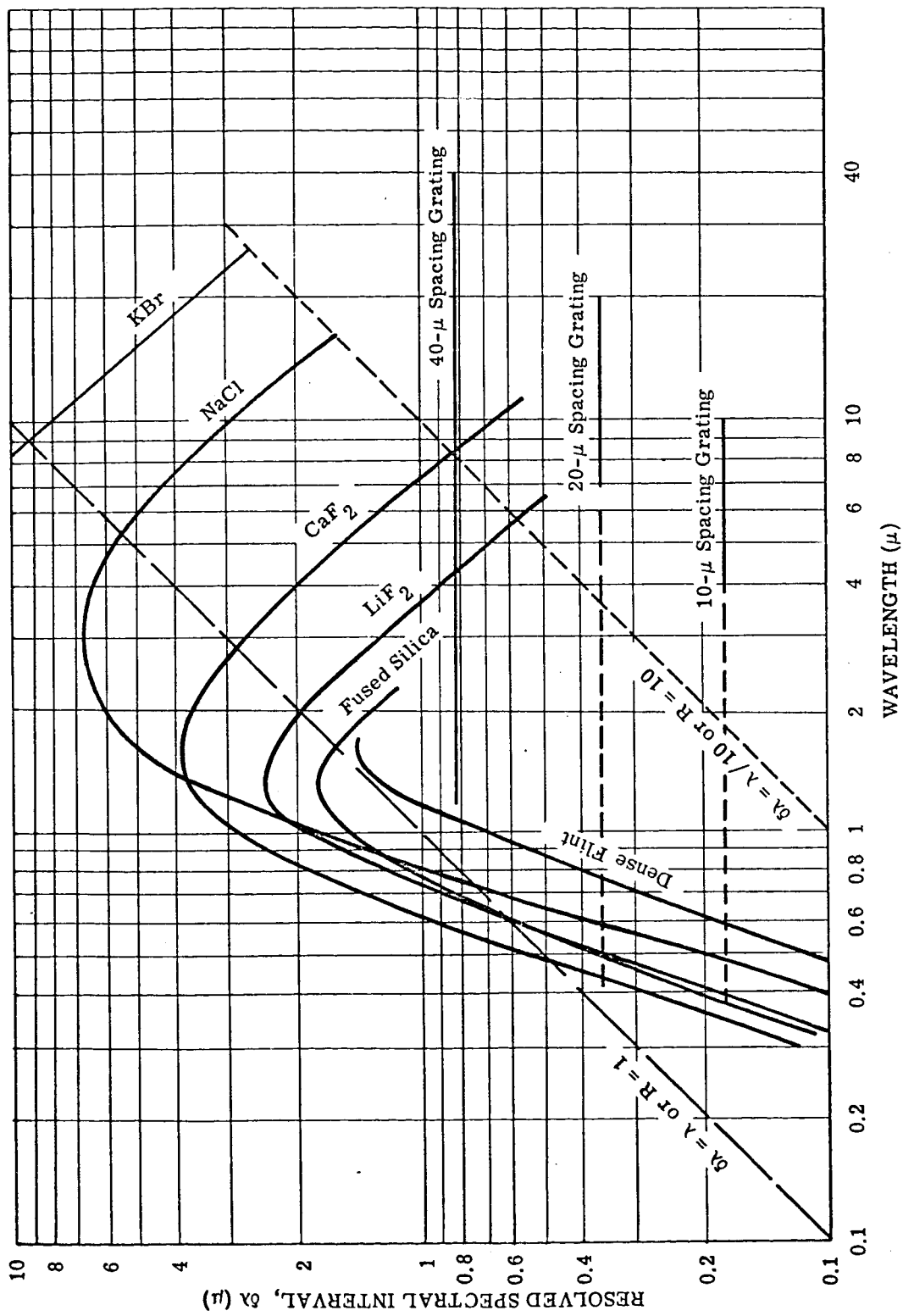

FIGURE 6. SPECTRAL RESOLUTION FOR VARIOUS DISPERSING ELEMENTS USED WITH SYSTEM GEOMETRY GIVEN ON PAGE 12

3.2. DETECTORS AND ASSOCIATED OPTICS

3.2.1. PHOTOMULTIPLIERS FOR THE 0.3-0.8-μ REGION. Photomultipliers are the most sensitive and convenient detectors available for the 0.3-0.8-μ region. They do, however, have two disadvantages: The need for high-voltage bias supplies, and the relatively large sizes and sensitive areas of conventional tubes.* The former is an engineering problem presenting no difficulties of principle. The latter means that it is not possible to use these detectors in close array form as can conveniently be done with photoconductive detectors. The individual detectors must be coupled to the dispersed spectrum by optical means. This problem might be solved by systems of mirrors, but a much more convenient technique is the use of light pipes (fig. 7). These pipes could take the form of fiber optics bundles or of solid dielectric rods. Use of fiber bundles, which are flexible, facilitates design and assembly. On the other hand, the rods are stiff and somewhat brittle, though they can be preformed to any desired shape not involving sharp bends. They would, however, have higher transmission efficiencies by about a factor of 2 relative to fiber bundles. In carrying out the calculations used to develop figure 17, it was discovered

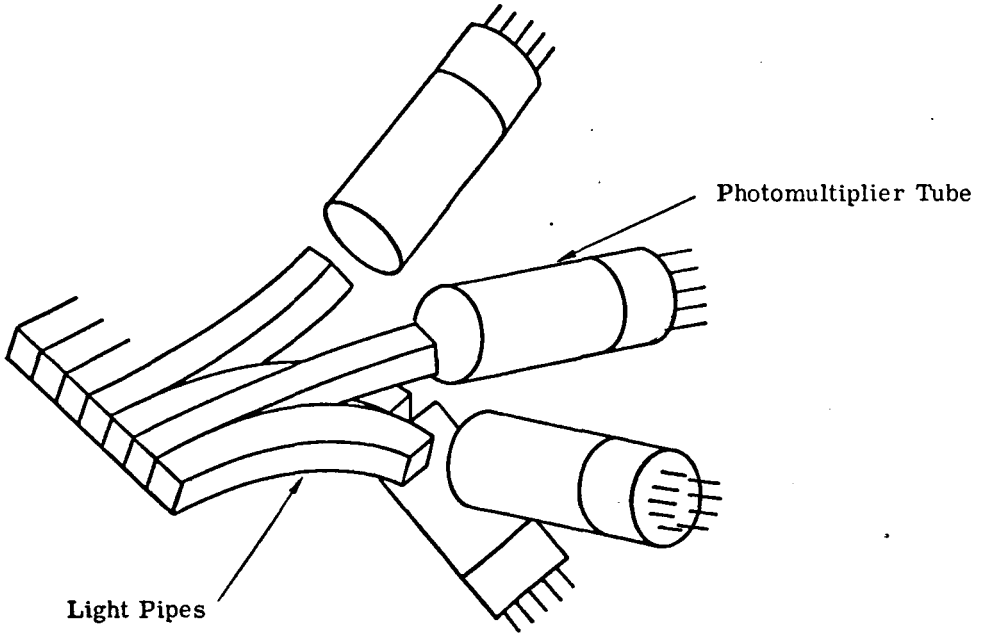

FIGURE 7. LIGHT-PIPE SYSTEM

*Experimental photomultipliers the size of hyperdermic needles are currently under development by the Bendix Corporation but were not considered as state of the art.

that the dark currents associated with photomultipliers and the noise associated with these dark currents can be ignored. As a result it is not necessary to minimize the detector area (as must be done when using semiconducting detectors) by minimizing the f-number of the beam at the photocathode. As a result, efficient management of the f-numbers involved in the optical coupling of the light pipes to the photomultiplier tubes is not required. It is, of course, desirable to keep transmission and reflection losses as small as possible. It will probably be satisfactory to position the photomultiplier tubes such that their windows are close to and facing the ends of the individual light pipes.

3.2.2. InAs DETECTORS FOR THE 0.8-2.6-μ REGION. As seen in table II, the time constant required for detectors must be about 10 to 20 μsec to match the dwell time. Unfortunately, this precludes the use of uncooled PbS detectors, and liquid-nitrogen-cooled InAs detectors become the choice, with the best sensitivity for this wavelength region.

3.2.3. InSb DETECTORS FOR THE 2.6-6-μ REGION. Similarly, InSb is the best detector choice for the 2.6-6-μ region and like InAs requires liquid nitrogen for cooling. In the airborne system, a cryogenic liquid transfer system would appear to be the most satisfactory of the various available systems. However, modern closed-cycle cooling systems are proving very satisfactory and are a more expensive but in many ways more convenient alternative, particularly for short arrays.

3.2.4. Ge:Cu DETECTORS FOR THE 8-25-μ REGION. The requirement of 8-25-μ operation of the scanner places a severe limitation upon the choice of detectors. Ge:Cu is probably the best choice, since it offers nearly background-limited sensitivity with an effective cutoff wavelength of 25 μ. Its peak D^*_λ value is 2.5×10^{10} cm-cps$^{1/2}$-w^{-1} (at 23 μ) at an operating temperature of 4.2°K (liquid helium). The detector maintains this sensitivity up to temperatures as high as 16°K, reaching its optimum at 12°K (see fig. 8).

Sensitivity (detectivity, D^*) can be increased by a factor of 2 at all wavelengths by cold shielding the detectors. Detectivity at shorter wavelengths can be improved by providing cooled long-wavelength cutoff filters for the detectors. It is desirable that a 16-μ cutoff filter be provided for the 8-14-μ channels to eliminate excess background noise, otherwise the performance in these channels would be only half as good as could be obtained with Ge:Hg at 28°K. Ge:Hg would in fact be the preferred detector if the wavelength range is restricted to the 8-14-μ band.

For an airborne application, a liquid helium transfer system would combine minimal cost and minimal complexity for cooling the detectors, though a closed-cycle system would be competi-

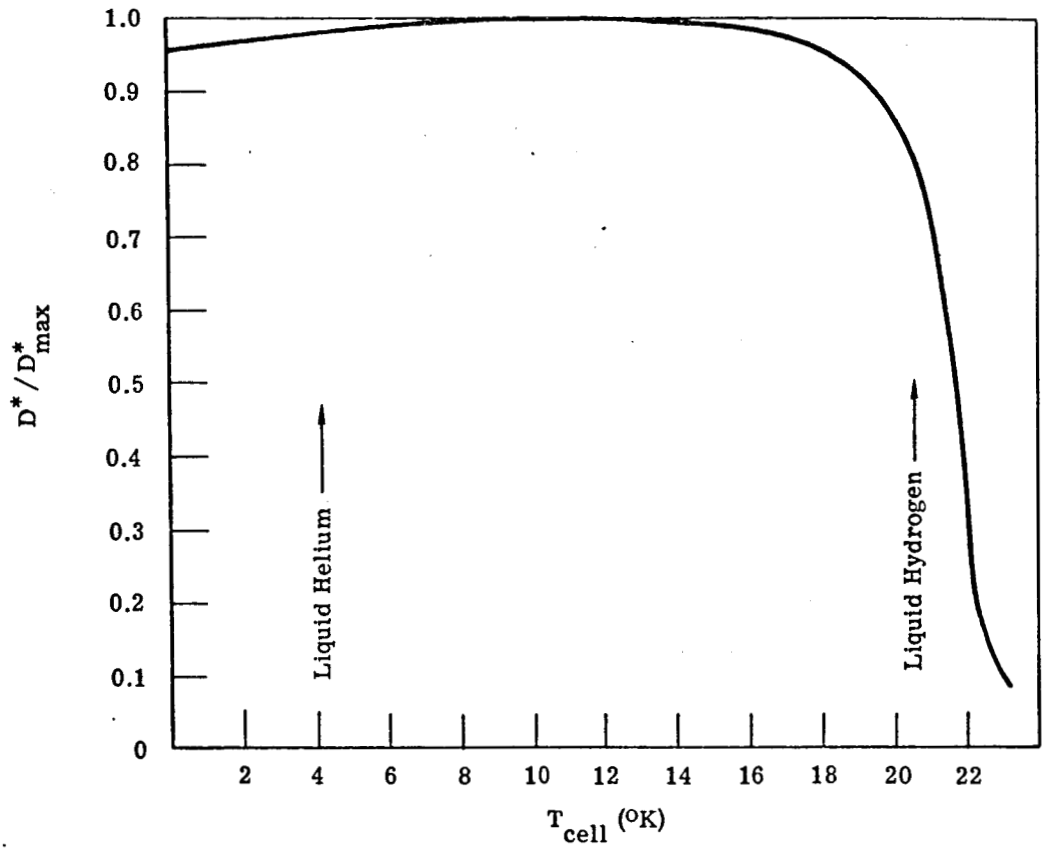

FIGURE 8. DEPENDENCE OF D* ON CELL TEMPERATURE, Ge:Cu DETECTOR

tive and more convenient under some circumstances. The exact design of the cooling system would depend in large measure upon the final configuration of the detector elements.

The importance of maintaining a stable detector cell temperature for qualitative measurements is illustrated in figure 9. At liquid helium temperature, a variation in cell temperature of $\pm 1^{\circ}K$ will cause an apparent change in target emittance of by $\mp 0.5\%$. At liquid hydrogen temperature, a $1^{\circ}K$ cell temperature variation would indicate a variation of $\pm 25\%$. For a 6-mrad orbital system the electronic bandwidth will be on the order of 1.8 kc. This bandwidth is relatively narrow and so should present no difficulties in preamplifier design.

3.2.5. FIELD LENSES FOR SOLID-STATE DETECTOR ARRAYS. In general, the sensitivity of detector-noise-limited systems is optimized when the f-number of the cone of radiation falling onto the detectors is minimized so that the detector itself can be made as small as possible. As explained in section 3.1, the f-number of the beam at the exit slit array of the spectrograph may be specifically larger than the theoretical limit of 0.5 or the practical limit,

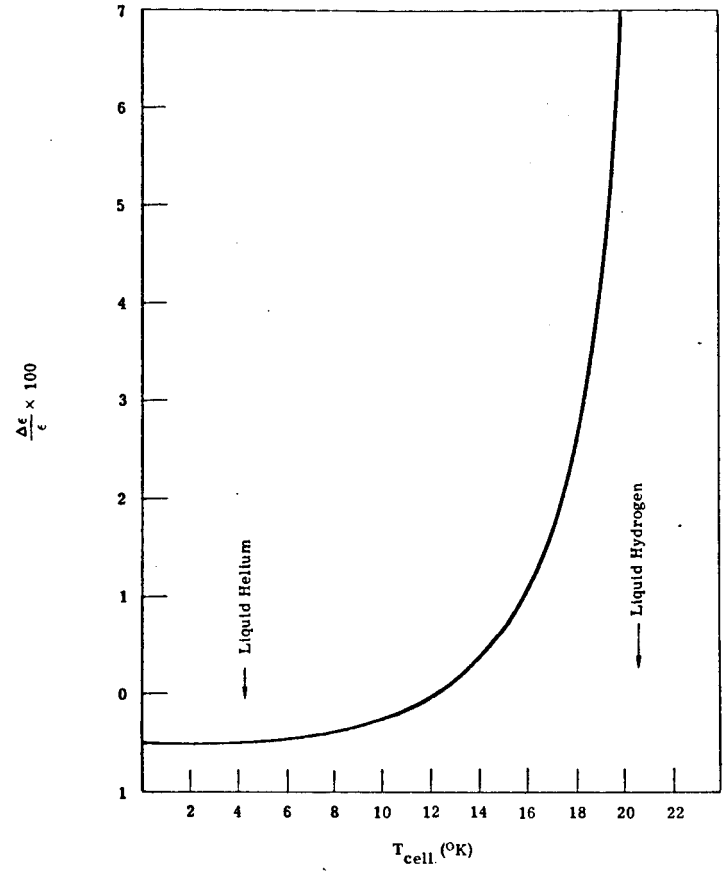

FIGURE 9. APPARENT CHANGE IN TARGET EMITTANCE CAUSED BY 1°K CHANGE IN DETECTOR CELL TEMPERATURE, Ge:Cu DETECTOR

which is usually between 0.5 and 1. Use of a condensing lens system to reduce the f-number of the beam would present formidable design problems and hardly seems feasible. An alternative approach is the use of fast field lenses in the focal plane of the spectrograph with the detectors located at the image of the prism or grating formed by each field lens. Comparable systems with and without field lens are shown in figure 10. It will be seen that individual detectors are reduced in size but that the total length of the array and thus the area which must be cooled is not. Field lenses provide two important incidental advantages, however. First, as will be seen by inspection of figure 10, cold shielding and filtering can be provided both more easily and more effectively if field lenses are used. The reason is that each field lens is a stop for all rays reaching its detector, whereas no such stop exists close to the detectors if field lenses are not used. Second, the usual spacing between the detectors when fields lenses are used will facilitate provision of both adequate electrical insulation and shielding between the detector elements and the necessary electrical connections to the elements.

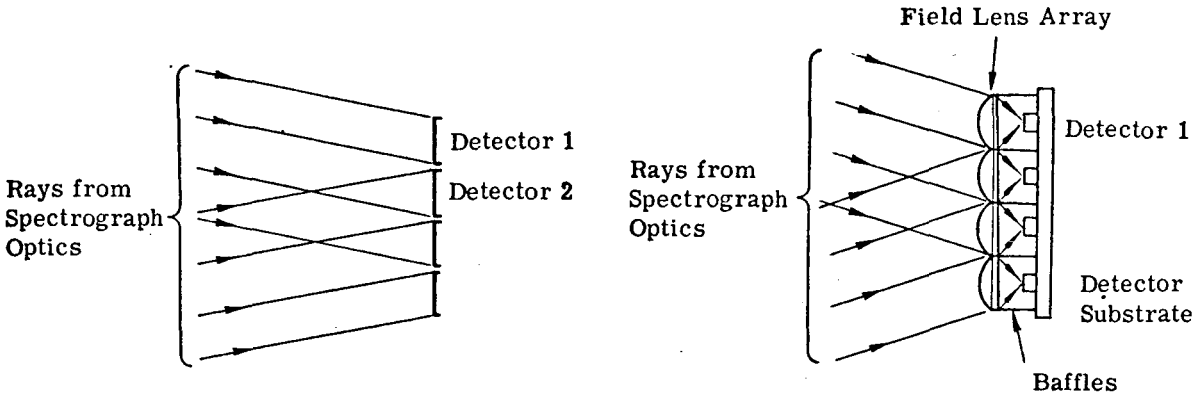

(a) Non-Field-Lens System

(b) Field-Lens System

FIGURE 10. SPECTROGRAPH SYSTEMS WITH AND WITHOUT FIELD LENSES

3.3. DATA PROCESSING

Printing out as a strip map the information contained in the video signal in one detector channel will be a straightforward operation, essentially similar to that used with conventional airborne scanners. In the same way, any linear combination of the signals in the various spectral channels can be printed out to make a strip map. In simple cases such a map can contain all the information that is needed. In general, however, the situation is much more complex.

Two rather different modes of operation need to be distinguished. In the first place the proposed orbital and airborne instruments might be used as research instruments to investigate what can be discovered about the terrestrial and lunar surfaces by such techniques. Second, more advanced systems could be used for routine compositional mapping of these surfaces by matching the measured spectra against a relatively small library of preselected spectra.

In the former case it is clearly desirable to store and transport all the data for later analysis. Reduction of the data bulk, if essential, should only be done either by limiting the periods of data gathering by some form of prediction or by on-board editing by an astronaut to reject uninteresting data. The analysis of the data would most likely be some type of regression analysis in a general-purpose computer. In this type of analysis a class of library spectra is fitted to the experimental data in some sense, e.g., in the "least square" sense [1, 2]. In this manner some quantitative measure of the relative proportion of each of the library materials existing in the sample being analyzed can be derived.

For mapping operations it must be assumed that some a priori information exists as to the type of material to be expected and the distribution of these materials. If the surface to be mapped is a heterogeneous mixture (within one resolution element of the scanning device) of

several of the materials being sought, then the data processing would most likely consist of correlating stored library spectra of those anticipated materials with the incoming data. This would provide a measure of how well the data "fits" the several library spectra.

The spectrum with the highest cancellation coefficient would be announced as the most likely constituent of the surface being measured. The relative ordering of the correlation coefficients obtained in this manner might convey useful information as to the relative percentages of various materials; however, this is conjectural at the present time.

If it is known that the surface is homogeneous in that principally one material constitutes the surface being measured for areas larger than one resolution element of the instrument, the decision-oriented processing can be implemented.

In the absence of useful a priori information it is possible that some sort of adaptive processing could be used. Processing of this sort would undoubtedly be involved if the recorded data is processed on a general-purpose computer, though the adaption might well be done by the intervention of human intelligence rather than automatically. However, the development of an adaptive processing system for on-board use would be a major undertaking and consideration of such a system is felt to be beyond the scope of this report: such a system would represent a considerable development in the state of the art.

Multispectral decision techniques have two types of limitations. The first is rather obvious: even in the absence of noise, unambiguous decisions will be possible only if all the spectra of the class of material to be recognized are distinguisable from those unwanted. To understand this statement it is best to think of any given spectrum as represented by a multidimensional vector of which each orthogonal component represents the spectral intensity in one resolved interval of the original spectrum. Thus if the spectrum is measured in N resolved intervals, one vector space will have N dimensions. When the vector corresponding to a sample of some class of material is plotted in such a space it will be possible to enclose the points representing those vectors in one or more surfaces; and unless the sampling was inadequate it will be possible to distinguish objects of the class represented from any object whose spectrum-vector does not end inside the volume so defined. Thus these limitations must eventually be determined experimentally. Obviously the more spectral intervals that can be used the more dimensions each vector will have. Thus a smaller fraction of the available hyperspace will be included in the hypervolume enclosing the class of target spectrum (provided that noise affects can be ignored). In this way the a priori probability of distinguishing classes is increased by using more spectral intervals. It should also be noticed that variations in reflected spectral intensity due to changes in illumination intensity, illumination angle, or observation angle will generally alter the magni-

tude rather than the direction of the corresponding vector. For emission spectra a similar effect would occur for changes in the temperature of the emitting material. In fact, the hypervolumes for such sets will tend to be elongated, hyperellipsoids lying along lines radiating from the origin. Other classes of spectra could be expected to belong to similarly restricted hypervolumes.

The second type of limitation is practical and is related to the fact that, as the spectrally resolved intervals are reduced in width, the S/N available will decrease and the processing system complexity will increase. The boundaries of the classification hypervolumes will become less and less definite if the S/N is reduced as the uncertainty in the location of each vector increases. Thus in some cases in which in theory the classification volumes can be separated by increasing the number of spectral intervals used, the poorer S/N resulting from the use of narrower interval with the best practical equipment may prevent recognition with the necessary certainty.

It should perhaps be added that in most practical systems absolute certainty is not required or obtainable. Thus the classification hypervolumes can overlap to the extent allowed by the permissible false alarm and miss rates.

It will be clear from the above that the complexity of the data processing system required for a particular purpose will vary considerably depending on the nature of the spectra of the material which is to be measured and classified. However, notice that three degrees of complexity can be illustrated by considering a simple case (fig. 11) in which measurements at only

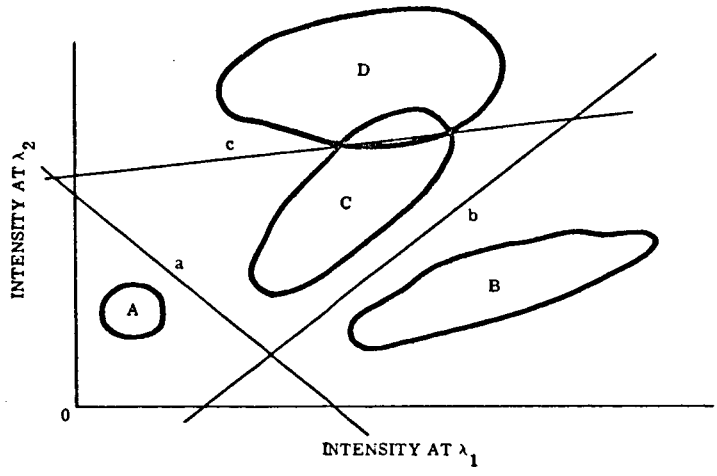

FIGURE 11. VECTOR REPRESENTATION OF FIELD DATA

two wavelengths are involved. The vertical hyperspace reduces to the positive quadrant (negative intensities are unknown since reflectance and emittance vary between 0 and 1) of a two-dimensional rectangular coordinate system. The extension to multicoordinates systems will be readily understood if the closed areas are thought of as representing closed hypervolumes and the lines as hyperplanes. In particular it should be remembered that a hyperplane in N dimensions can be represented by the equation

$$\alpha_0 + \sum_{i=1}^{N} \alpha x_i = 0$$

which is the equation of a line when N = 2.

In figure 11, A, B, C, and D are areas containing all the samples of noiseless spectra corresponding to four classes of material A, B, C, and D, respectively. The areas would reduce to points if there were no variance within a class of material. Lines a, b, and c are drawn to separate the four areas. Note that line c is to some extent arbitrary, because C and D overlap.

The simplest processing is that of distinguishing area A from the others. Line a can be represented by an equation

$$\alpha I_{\lambda_1} + \beta I_{\lambda_2} = \gamma$$

where I = intensity, in which each constant is positive. Thus if we form the weighted sum $\alpha I_{\lambda_i} + \beta I_{\lambda_2}$ for any pair of values known to belong to A, B, C, or D, then they, in fact, can belong to A if and only if this weighted sum is less than γ. This is a very simple operation to perform electrically and in fact is also the operation performed when a film-filter combination is used (the filter supplies the coefficients α, β, etc.).

A somewhat more complex process is required to distinguish B from C, D, and A because the equation for b has a negative coefficient. This presents no difficulty electrically, but cannot be implemented with film-filter combinations as in this case all coefficients have a positive value. In fact, it is clear that the film-filter technique can only distinguish between areas which can be separated by lines which intersect both axes on the positive side of the origin. Each line requires a separate film-filter combination.

The third level of complexity is represented by the differentiation of examples of C from D, A, and B. Neglecting the problem of overlap of C and D, we need to determine whether the target point is enclosed by a, b, and c, or not. We can determine whether or not the point lies on the correct side of each line individually as before, and then use "AND" circuitry to determine if it lies on the correct side of each line.

We can approximate any shape by a series of straight lines and avoid ambiguities due to reentrant shapes or isolated areas by considering the areas as having several component parts and using "OR" circuits to obtain the correct answer.

Thus any problem in which the representative hypervolumes are separated can be treated in this way, though it is clear that the electronic complexity involved will increase with both the number of dimensions (i.e., spectral intervals) involved and with the number and complexity of the hypershapes involved.

Further, it should be noticed that the introduction of noise will affect the certainty of the decisions made, but not the processing techniques, though it may destroy their practicability under unfavorable circumstances.

However, this study is primarily concerned with an airborne precursor for orbital experiments, so that resolution of questions about the complexity of the processing equipment is to some extent premature. Fortunately, the bulk of data which could be collected in a single aircraft flight presents no storage or transport difficulty, and we recommend that for such flights the raw video data be recorded complete and processed in standard general-purpose computers.

3.4. CALIBRATION AND SIGNAL LEVEL CONTROL

In the early development of optical-mechanical strip-mapping techniques no serious attention was paid to the problem of power calibration. In fact (as in general photography), because the information was carried in the shapes or patterns portrayed in the various shades of gray visible in the final image, the need for an absolute calibration of the gray scale was not necessary. Subsequently, as need for calibrated strip maps for quantitative tone evaluation, arose, calibration systems were added on an ad hoc basis. These generally took the form of collimated stable or standard sources which partially obscured the field of the scanner.

In a multispectral scanner in which the spectral information is carried in parallel detector-amplifier channels, relative calibration between the channels is essential; otherwise the array of output signals cannot be properly compared and distinguishing between a spectral absorption band and the effects of a low gain channel would, for instance, be very difficult if not impossible. For most applications in both the thermal and reflective regions absolute calibration is also highly desirable.

As explained in section 3.1, optical systems are not likely to employ very small f-numbers. Thus, it will be relatively easy to introduce calibration signals during the scanner dead times by means of a mirror chopper synchronized with the scan-mirror rotation mechanism. If this

chopper crosses the beam close to the spectrometer entrance slit where the beam cross section is small, it will be possible to make the switching time quite small. By use of similar and the same number of reflecting surfaces in the calibration beam as are used in the scanner itself, the problems associated with the relative optical efficiencies of both beams can be reduced to negligible proportions. One scheme using off-axis optics is shown in figure 12. If necessary more than one chopper could be used to introduce more than one reference source.

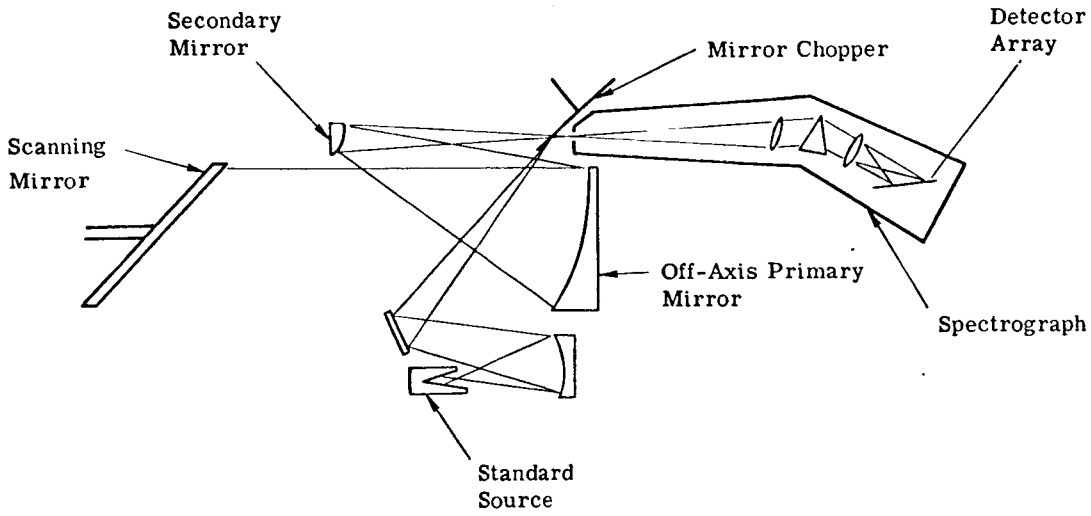

FIGURE 12. CALIBRATION SYSTEM WITH OFF-AXIS OPTICS

Variable radiance sources could be used in the form of filament or other types of lamps for the shorter wavelengths, and thermoelectrically controlled blackbodies for the longer wavelengths. If the calibrated source is adjusted to have a radiance close to the mean radiance of the scene and the mirror chopper is designed or the video signal is gated so that there is no time during which the scanner is looking at its own housing, the dynamic range requirements of the amplifier chains and recording channels can be greatly reduced. This dynamic range problem, resulting from the fact that the difference in radiance between the scene and the scanning mirror housing is often many times larger than the radiance range of the scene, has been a major problem with many airborne scanner systems. Often considerable complication of the electronic system has had to be introduced to reduce the signal handling problems to tractable levels. To illustrate the problem and the solution proposed above, representative video signals are shown in figure 13.

An alternative nonelectronic solution would be to control the temperature or radiance of the scanner housing. This, however, is a much more awkward solution: the housing whose radiance would have to be controlled would be quite large.

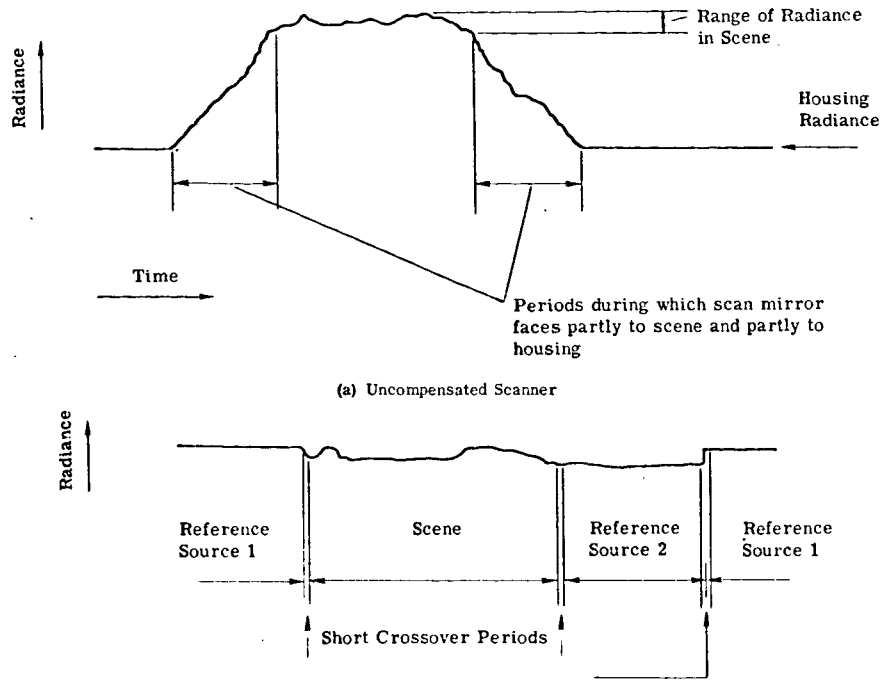

FIGURE 13. VIDEO OUTPUTS

3.5. SYSTEM STABILIZATION

If the platform (aircraft or spacecraft) on which the scanner is mounted rotates about a set of axes fixed relative to the target plane, the strip map produced will be distorted. It is, therefore, necessary to ensure that the platform roll, pitch, and yaw and their angular rates be limited to prevent excessive distortion of the image produced. Note that in practice an alternative to rotation stabilization exists: if the rotations and rotation rates are recorded continuously in synchonism with the scanner video signals, the distortions can be removed during data processing. In principle some underlap can occur if this is done, and although this cannot be removed by data processing such effects are of no moment in practice.

Suppose the scan lines are perpendicular to the direction of linear motion of the platform. If the rotation is a pitch (about a horizontal axis perpendicular to the motion) then the scanned lines on the target plane will remain parallel but their spacing will alter during the pitching motion producing underlap or overlap. If the rotation is a yaw (about a vertical axis) the scan lines will rotate with the platform but be undisplaced directly beneath the platform. For a roll (about the line of motion) successive scan lines will be displaced lengthwise relative to each other, producing a shearing effect on the image.

It should also be noticed that distortion of some kind is generally introduced in the process of converting the video signal from the scanner into pictorial form. As with photography, if the topography of the target surface is not known there may be considerable uncertainty of the location of the true object point at large scan angles. Thus, if the scanner is looking (instantaneously) close to the (mean) horizon, the true object may be a mountain top much closer to the platform, or a hillside at some intermediate position. However, if the topography is known, such effects can be calculated, at any rate in principle; and, perhaps more important, for scan angles of less than about 40% from the vertical they are generally negligible. The differences between the various possible projections of the video data into pictorial form are also negligible. A wide disparity may also be noticed between the scales of the strip map along and perpendicular to the flight direction if the film speed in the printout device is not correctly matched to the system's operating parameters.

Both these projection problems and the stability problems can be dealt with in exact mathematical terms, but the results are extremely complex. However, by assuming that the platform will be stabilized to within a few degrees and that only the central $\pm 40^{\circ}$ of the scan will be used for exact map matching, we can use relatively simple arguments to assess the stability performance required of the spacecraft.

Two types of alignment errors must be distinguished. The first constitutes continuous errors in which the scanner axis and vertical reference are permanently out of alignment with the platform track and the true vertical. For a constant roll or pitch error of ϕ_1 or ϕ_2, the strip map will be displaced by a distance αH (where H is the altitude of the platform) appropriately scaled from its true position. (Strictly this is only true for points directly beneath the platform and is only approximately true within the central $\pm 40^{\circ}$ of the scan.) Provided ϕ_1 is small (a few degrees) a permanent error of this sort will have no effect on the problem of matching the strip map to a geographical map based on photographs. In the case of yaw, map errors in the direction of flight will be introduced. They will vary with the ground distance of the image point from the subpoint of the platform, and their sign will change from one side of the subpoint to the other. Numerically the error will be $\phi_3 H \tan\alpha$, where ϕ_3 is the yaw angle and α the instantaneous scan position relative to the downward vertical. Since $\tan\alpha < 1$ for the central part of the strip map of greatest interest, we can write this error as $<\beta H$ and together with the earlier result for roll and pitch, say, that the map error will be $\sim\phi H$, where ϕ is the angle through which the platform has rotated about any axis from its normal position.

Thus if we require $\phi << \beta$, the angular instantaneous field of view, it will be impossible to detect map errors or distortion due to platform instability. However, such a tight tolerance will be unnecessary unless perhaps the scanner is being used for primary mapping, which is

unlikely. In fact, constant errors of the order of 2^{o} or even 5^{o} in an 80^{o} or 100^{o} strip would be of little moment for many applications.

Second, rapid changes of attitude of smaller amounts will be unacceptable because these will lead to lines and curves appearing wavy or even zig-zag on the strip map. The precise requirements on rotation rates will, of course, depend on the amount of small-scale distortion which is acceptable for any particular application. Generally, it will be adequate to require that rotation rates ($\dot{\phi}$) be less than one field of view in the time for, say, 10 scans; that is,

$$\dot{\phi} < \frac{\beta}{10(2\pi/\dot{\alpha})}$$

or, from equation 2,

$$\dot{\phi} < \frac{\beta}{20\pi} \times \frac{2\pi(V/H)}{n\beta}$$

i.e.,

$$\dot{\phi} < \frac{V/H}{10n} \qquad \text{(A)}$$

For the earth or lunar orbits of interest, $V/H \sim 0.025$, so that, taking $n = 3$, we find

$$\dot{\phi} < 0.025/30$$

or about 1 mrad/sec. Thus our preliminary recommended stability requirements for the orbits is to limit rotations from normal flight altitudes to not more than, say, $2\ 1/2^{o}$ with rotation rates less than 1 mrad/sec. Such performance can probably be expected of the spacecraft, and no further stabilization will be required. Similar performance would be required of the airborne prototype. However, aircraft tend to be relatively stable in yaw and pitch, whereas roll stabilization can be introduced into scanner readout mechanisms fairly readily. Thus for the airborne prototype installation, roll stabilization to comply with equation A is required.

4
LUNAR GEOLOGICAL SURVEYING FROM LUNAR ORBIT

4.1. SYSTEM TRADE-OFFS AND PERFORMANCE

It has been known for many years that the reflection spectra of minerals show characteristic reststrahlen bands in the infrared. Various authors ([3, 4, 5]) have pointed out that a qualitative identification of geological surface composition should be possible by utilization of this property of the constituents of rocks. Under favorable surface conditions and with a spectral resolution of 5 cm^{-1}, major rock types could be readily identified by their diagnostic spectra in the 8-25-μ wavelength range, or even the 8-14-μ range. However, it has been postulated on

the basis of several converging lines of evidence that the surface of the moon is less than ideal for this type of measurement, because it is composed of a finely powdered material (experiments indicate that spectra show diminishing detail as particle size is reduced). Taking this into account, it has been shown that differentiation of felsic and mafic rocks is still possible (for particles of about 100 μ in diameter [5, 6] and even 10 μ [7] in diameter) with a spectral resolution of 40 cm^{-1} (0.4 μ). Hovis and Callahan [5] have determined that, in the 1-4 μ region, reflectance increases with decreasing particle size. Thus, measurements in this region might be used to resolve ambiguities arising from lack of knowledge of particle size.

An orbital infrared survey of the earth's surface for geological purposes encounters difficulties not found in a lunar survey. The presence of an atmosphere limits the survey to appropriate "windows" of high transmission. Vegetation, soil, and glacial deposits overlie and obscure many of the relationships geologists seek to understand. Nevertheless, recent imagery taken by the NASA meteorological satellite Nimbus I indicates that elucidation of some features is possible [8]. Examples of experiments which appear feasible are: (a) detection of temperature anomalies due to local climatic differences; (b) discernment of topographic lineaments and regional stratigraphic and structural patterns; (c) mapping of volcanic thermal patterns. If spectral information is available, we can add the determination of rock type based upon reststrahlen wavelength. In the light of present knowledge, the relatively narrow 10-12-μ band is most favorable for use in these studies as measurements in the wings of the 8-14-μ atmospheric transmission band would be highly confused by the effects of the absorption and emission lines occurring there. The 10-12-μ band in fact offers good atmospheric transmission, a maximum in the earth's radiant energy spectrum; and also some spectral information related to the chemical composition of the surface rocks.

The instantaneous angular field of view will determine the spatial resolution at the surface. Although high resolution is desirable from the point of view of isolation of small independent features, it will generally lead to a high data rate, high data bulk, and low sensitivity. Reducing the spatial resolution, on the other hand, although generally giving higher sensitivity and lower data bulk and rate, will also imply a physically larger system. In the following example, a value of 0.0067 rad has been used; this seems to be a convenient compromise. This value leads to a spatial resolution at the lunar surface of 0.5 km for a 75-km orbit, so that all features visible in terrestrial observations would be resolved. For a terrestrial orbit, the surface resolution would be three or more times larger because of the higher orbits which must be used by earth satellites.*

*A finer spatial resolution would be desirable for terrestrial applications. This could be achieved by relaxing some of the other specifications or possibly by the method indicated in section 7.5.

A multispectral scanner with a resolution of 0.4 μ in the 8-14-μ region (15 output channels) would be a reasonable and useful device provided it had adequate sensitivity. To find out, we use the appropriate S/N equation (eq. 12).

Assuming a 75-km-altitude lunar orbit or a 300-km earth orbit, we can put V/H = 0.025, and by proposing a straightforward but efficient scanning system we can assign reasonable values to many of the parameters as follows:

n = 2

m = 1

F = 1

β = 0.0067 rad*

o.e. = 0.3

s.e. = 0.5

D^* = 2×10^{10} for a Ge:Hg or Ge:Cu detector efficiently cold shielded and filtered for for 8-25 μ

S/N at least 5 if we are to make decisions on the spectra from a single spatial resolution element

Figure 14 shows the spectral radiance (N_λ) of blackbodies at various temperatures corresponding to those typical of various parts of the moon's surface, plotted against the range of wavelengths of interest. Most of the warm face of the moon, and almost all the earth's surface, is hotter than 240°K; therefore, we can take $N_\lambda = 2 \times 10^{-4}$ w-cm^{-2}-sr^{-1}-μ^{-1} as a lower limit to the spectral radiance in the 8-14-μ region. Then, choosing the minimum differential emittance that we need to observe as $\delta\epsilon = 0.01$, and substituting all these values in equation 12, we find the necessary diameter of the collector mirror to be

$$D_1 = 15 \text{ cm}$$

which is quite practical. A schematic optical layout for such a scanning system is given in figure 15.

Addition of a single relatively wideband channel in the 1-2.5-μ region to measure solar reflectance would give some indication of particle size, as mentioned above. This could be done by the beamsplitting method shown for the Ge:Hg channel in figure 16. For the terrestrial case, the 1.5-1.8-μ band (which is relatively free from absorption) would appear to be optimum.

Extending the system to cover the whole 8-25-μ range involves no intrinsic loss of sensitivity, though the lower lunar radiances at 25 μ would make the observable $\delta\epsilon$ at these longer

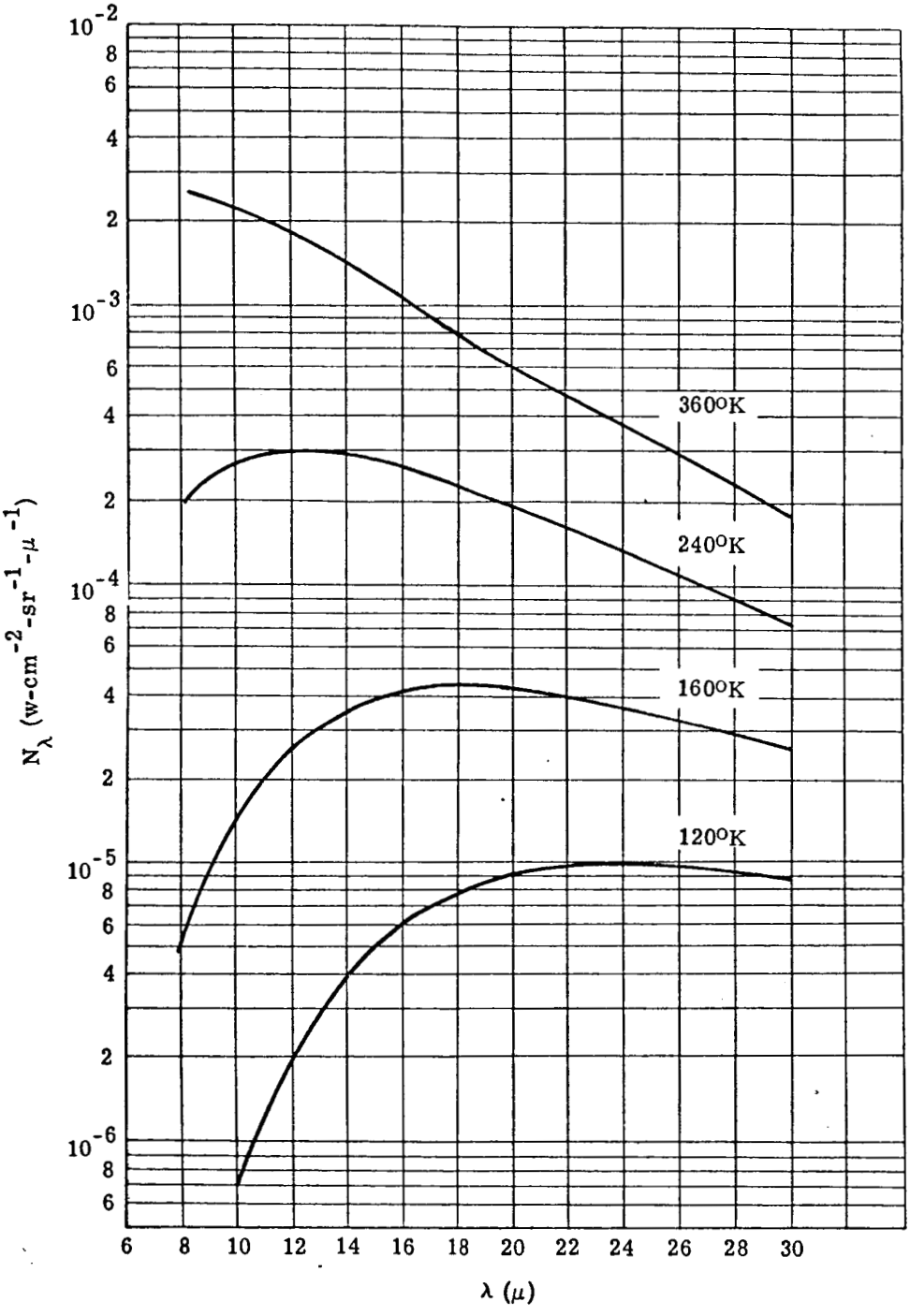

FIGURE 14. BLACKBODY SPECTRAL RADIANCE. Various temperatures in the range occurring at the lunar surface.

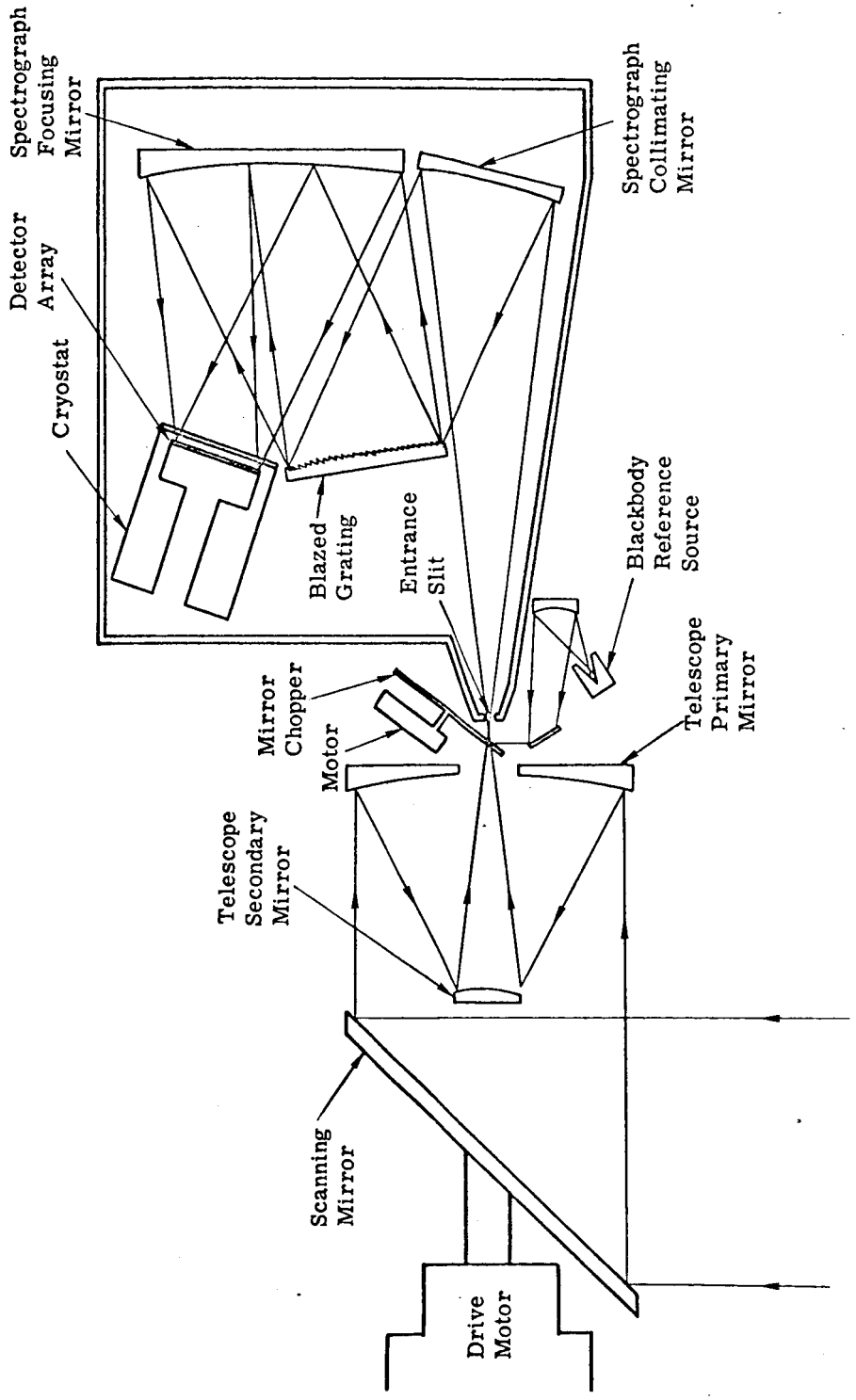

FIGURE 15. SCHEMATIC OPTICAL LAYOUT FOR LUNAR SURVEYING SENSOR

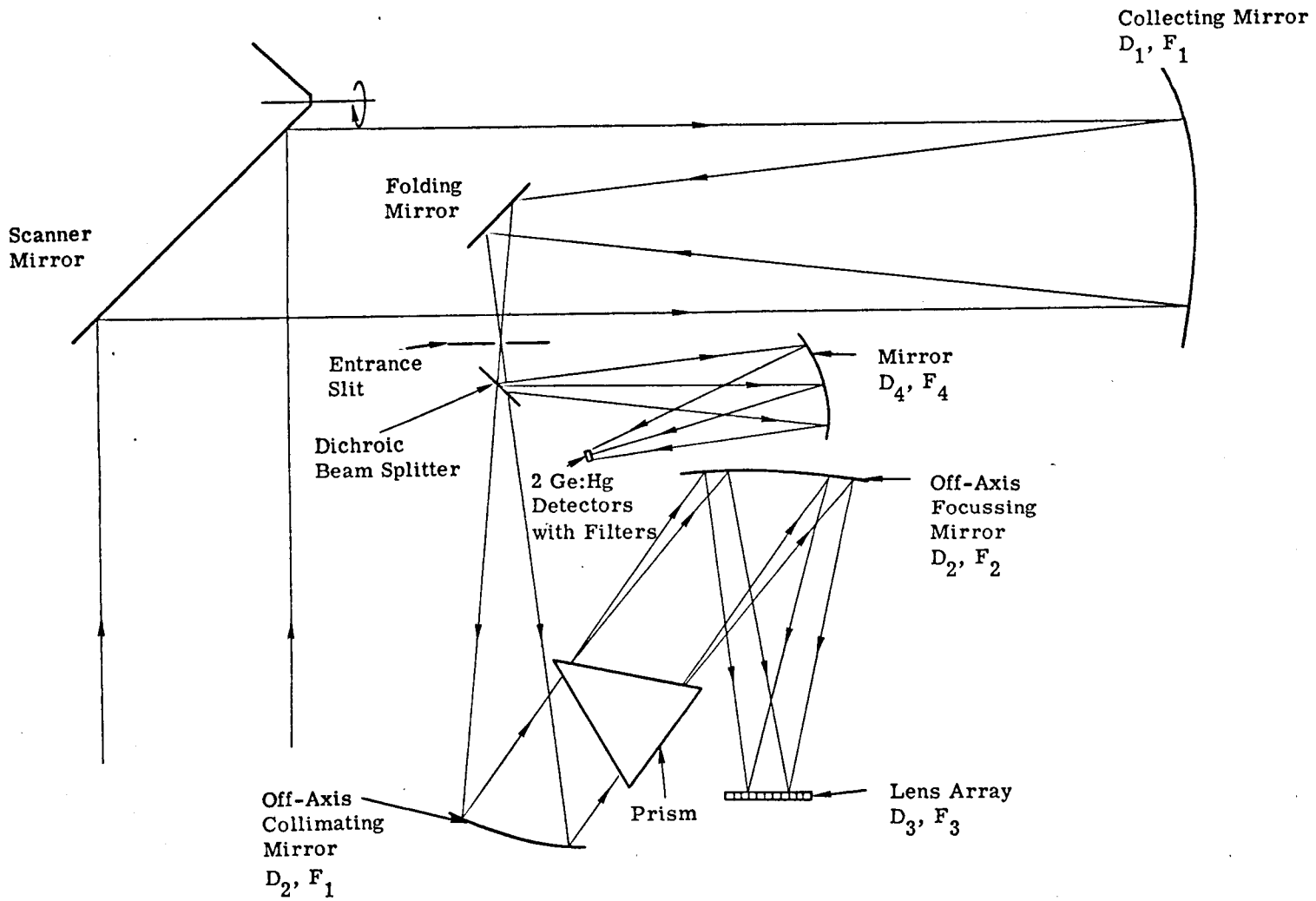

FIGURE 16. OPTICAL SCHEMATIC OF THE SCANNER-SPECTROGRAPH SYSTEM

wavelengths slightly greater than in the 8-14-μ region. Again, design of a wider wavelength-range instrument involves no difficulty of principle. In practice, however, lower overall grating efficiency would obtain if the wider spectral range were covered in a single grating. Also, the problem of providing an adequate cryogenic system for a detector array nearly three times longer would require considerable engineering. Separate spectrographs for the 8-14-μ and the 14-25-μ regions, with a single scan mirror assembly, might be preferable. The two entrance apertures could be put adjacent to each other, with folding mirrors separating the location of the two spectrographs in the focal plane of one telescope. Alternatively, the scan mirror assembly could be made double sided with a telescope and spectrograph facing each side. If necessary a wideband detector could also be integrated with the system to give a more sensitive wideband output in the 8-15-μ band to obtain thermal pictures with wide dynamic range of the warm side of the moon, and in the 15-25-μ band for the cold side.

4.2. DATA PROCESSING

Some of the gross features of processing data obtained from a scanning spectrometer such as that described in section 4.1 are discussed below. The type of data processing required depends on the amount of a priori information about the surface to be measured, as discussed in section 3.3. We assume that little or no a priori information is available, so that onboard processing would be difficult. However, a great deal of experimental work is being carried out on the spectra of rocks and minerals both in the laboratory and in the field, and this assumption and conclusion may well have to be changed in the near future.

The data could be transmitted to the earth in real time via a radio-frequency transmission system. The information would then be stored on earth in a convenient form, and the processing would be done in a general-purpose computer. For transmission, the data would be converted to binary form. Assuming a sampling rate of 4 times the maximum video frequency and quantization to 7 bits, the transmission bandwidth bw required is:

$$\text{bw} = N \times 4 \times 7 \times 4 \times 10^3$$

$$= 1.12N \times 10^5 \text{ bits/sec}$$

For a reasonable number of channels and the addition of any error-counting coding, the rate would probably be too high for the spacecraft system to telemeter in real time. Alternatively, all the raw data could be retained on magnetic tape in the spacecraft. The returned tape could be processed on earth-based computers, as stated above. If the orbiting instrument is designed so that the dynamic range of the tape machine could be handled by the tape machine (AGC), then the data could be recorded in analog form, permitting a higher information density

on the magnetic tape than with digital recording techniques. To compute the amount of tape required, assume that the mission length is 14 days; that maximum data are recorded at all times during the mission; that all N channels can be recorded in parallel on one tape; that each reel is 3600 ft long; and that the tape density is 3×10^3 c-in^{-1}. Then

$$\text{Recording time/reel} = 3600 \times 12 \times 3 \times 10^3 \times (4 \times 10^3) \times 3600^{-1} = 10 \text{ hr}$$

It appears unnecessary to record all the raw data continuously since the maximum rate of recording will probably take place only on the sunlit side of the lunar surface or specified parts of the earth's surface. Further reduction could be obtained by recording only target areas of interest and by not recording areas passed over more than once. Further, some in-flight editing by trained astronauts could be used as a major data compression method if needed. Thus for a 14-day flight, perhaps as many as 10 reels of raw data would have to be returned to earth.

5
GEOLOGICAL AND AGRICULTURAL SURVEY FROM EARTH ORBIT

5.1. SYSTEM TRADE-OFFS AND PERFORMANCE

Many orbital experiments of value to agricultural scientists have been surveyed in a recent publication (9). This report demonstrates the great interest in spectral analysis of solar radiation reflected from many kinds of terrestrial features. The wavelength range of prime interest is 0.3 to 2.5μ. Operating in the 2.5-8-μ region is marginal because of the excessive interference by atmospheric absorption and thermal emission. It seems probable that an instrument with a spectral resolving power R ($=\lambda/\delta\lambda$) of about 10 could obtain much valuable information. For many general surveys, a ground resolution of about 1000 ft would suffice. Current components can obtain this resolution from orbit. However, if individual objects such as trees, buildings, or animals must be resolved, much finer resolution would be required. With current components this would necessitate the use of a very large instrument capable of producing data at so high a rate that it would be extremely difficult to handle.

For detecting targets at temperatures above normal ambient, a 4.5-5-μ wideband channel would be optimum. Forest fires and volcanic phenomena are of interest in this category. Preferably the ground resolution should be 20 ft, with notification in near real time (for fires). As explained above, such fine ground resolution is not compatible with that likely to be obtained from orbit at present. However, even with a much poorer groung resolution, the larger fires should be resolvable and many smaller ones detectable as point sources. The same might be true for volcanic features.

A 10-12-μ wideband channel would be optimum for measuring the radiance temperatures of surface features. The spectral band from approximately 10 to 12 μ is chosen to minimize the attenuation and emission effects associated with atmospheric ozone, water vapor, and carbon dioxide. The system would be capable of detecting temperature differences of less than $1^{\circ}K$.

5.1.1. PERFORMANCE EVALUATIONS. In order to determine a reasonable set of parameters for the 0.3-2.6-μ system, two sets of parameters were evaluated. The two sets are called case I and case II, their basic parameters being listed in the first six rows of table II. This wavelength range can be covered satisfactorily with a fused silica prism, but would require at least two gratings with the attendant order-sorting filters. The discussion is therefore based on the use of a silica prism.

TABLE II. PARAMETERS FOR THE PRISM SYSTEM*

Parameter	Symbol	Units	Case I	Case II
Field of View	β	rad	1×10^{-3}	6×10^{-3}
Diameter of Collecting Mirror	D_1	cm	15	5
Resolving Power	R		10	10
Focal Ratio	F_1		6.67	6.67
Focal Ratio	F_2		6.67	6.67
Focal Ratio	F_3		1.0	1.0
Prism Aperture	D_2	cm	6.5	15
Dwell Time	τ	μsec	16	573
Slit Width	d_1	mm	1.0	2.0
Detector Width	d''	mm	$0.261 \leqq d \leqq 0.814$	$0.522 \leqq x_d \leqq 1.62$
Number of Faces on Scanner Mirror	η		2	2
Approximate Diameter of Scanner Assembly		cm	40	17
Prism Material			Fused quartz	Fused quartz

*Detectors are (1) S20 photomultipliers for the 0.3-0.8-μ region
(2) InAs (liquid nitrogen cooled) for the 0.8-2.6-μ region

For each case, the parameters listed in the first six rows determine the remaining parameters through use of the parametric equations derived in the appendix and discussed in section 2. (The focal ratio F_3 is always 1 because lenses with focal ratios <1 are very difficult to design.

The case I system uses $F_3 > 1$ at some wavelengths in order to obtain a detector no smaller than the minimum manufacturable size.) The measurable change in reflectivity for average daylight illumination is plotted in figure 17.

Calculations show that the necessary sensitivity in the two broadband channels can be readily obtained for systems with scanning parameters compatible with the multispectral system described.

5.1.2. SYSTEM DESCRIPTION. A possible optical schematic of the scanner-spectrometer system is shown in figure 16; no attempt has been made to arrive at the optimum design configuration. A dichroic beam splitter is used to pass the energy in the 0.3-2.6-μ band and reflect the energy from 4.5-5.5-μ and from 10-12-μ. The energy in the 0.3-2.6-μ band is collimated by the mirror D_2, F_1, dispersed by the prism, and focused by the mirror D_2, F_2, on the lens array D_3, F_3. The size of each lens in the array is chosen to intercept the energy in a given spectral resolution element; each lens in the array then focuses this energy on a given detector. Photomultiplier tubes are used as the detectors for 0.3-0.8-μ band, and photovoltaic InAs detectors are used for the region from 0.8-2.6-μ. The mirror D_4, F_4 focuses the energy in the 4.5-5.5-μ band and in the 10-12-μ band on cooled Ge:Hg detectors. Filters can be placed on these two detectors to pass only the narrow spectral bands of interest.

Of the two systems studied, case I is clearly the most satisfactory. It has an adequate signal-to-noise ratio, and the ground-resolution element size is quite large but still small enough to meet many requirements. The case II system has a ground-resolution element that is too large to be of much use.

With current technology, a first-generation system similar to the case I system ($\beta = 10^{-3}$ rad with ground resolution = 1200 ft, D_1 = 15 cm, and R = 10) could be packaged into an earth-orbiting satellite and would undoubtedly obtain much useful information. It is probable that advances in technology during the next few years will make systems with finer ground-resolution elements feasible.

5.2. DATA PROCESSING

The anticipated input to the data processor is a low-pass electric signal with a bandwidth of up to 100 kc. With the large number of channels being considered, the data rate appears to be excessively large for continuous recording or continuous transmission to earth.

Thus, it will be necessary to restrict severely the volume of raw data collected or alternatively to use some form of automatic real time data processing to compress the data bulk prior

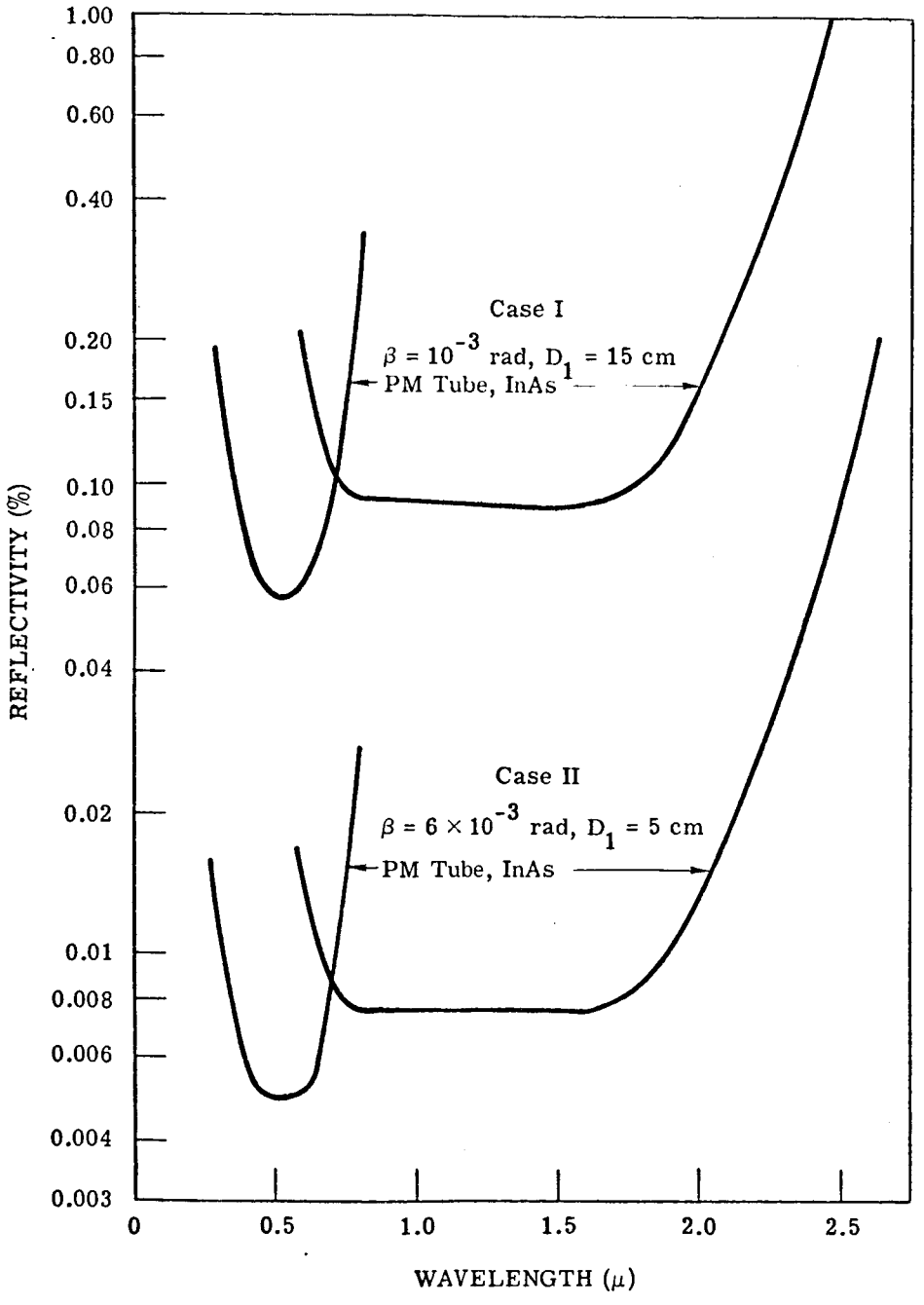

FIGURE 17. DETECTABLE PERCENT REFLECTIVITY

to storage or telemetry. In order to establish such a preprocessing system, it will be necessary to define a statistical data band. In view of the extensive and relevant data collection programs now being carried out, it should be possible to define a suitable data bank in the near future.

6
AIRBORNE SYSTEMS

Prior to orbiting and using the multispectral scanner equipment discussed in section 4 and 5, it will be highly advisable to use similar equipment in aircraft. Such flights would provide valuable development tests for the equipment itself and an understanding of the operating problems involved in its use. Equally important would be the preliminary verification of the value of multispectral techniques in various applications and investigation of the various calibration and data processing problems which arise in such applications. It should not be forgotten that such an airborne system would have considerable intrinsic value as a data collection system. In fact, it is likely that for applications in which fine ground resolution is of more importance than wide synoptic coverage, airborne rather than orbiting platforms are to be preferred.

6.1. RECOMMENDED SPECIFICATIONS

In either earth or lunar orbits, mapping devices will be operated in low-altitude orbits to obtain the best possible ground resolution, and thus in both cases will operate at a V/H of close to 0.025 rad/sec. By use of low-performance aircraft, this can be simulated at relatively low altitudes (10,000 ft for a ground speed of 200 mph) or by using correspondingly higher performance aircraft at higher altitudes. Thus the specifications for systems designed primarily for orbit could be used for the airborne precursory system. Unfortunately, the two systems are not compatible in that it is not possible to use a single scanner-single spectrometer combination to cover the two spectral ranges and the two recommended instantaneous fields of view simultaneously and efficiently (see eq. 2 and 5b). For many purposes, the use of separate instruments for the short-wavelength (0.3 to 2.5 μ) and long-wavelength (8 to 14 μ) applications would be the most sensible solution. In fact, if either system were developed for orbital use, prototypes in airborne experiments would be highly desirable both from the point of view of development testing and of making exploratory measurements with the systems.

However, from other points of view it is desirable to consider the feasibility of a system which would operate satisfactorily in both wavelength ranges simultaneously. The principal

value of such a system would be to investigate the relationships between solar reflection and thermal emission spectra for all classes of targets. Although this can be done by comparing strip maps made at various wavelengths by different scanning systems, it is much more satisfactory to gather the information simultaneously from a single optical system. This is particularly true if any type of electronic processing is to be used, because the spectrum of each field point is immediately available in electronic form. Otherwise, if separate scanners are used, strip maps made with each scanner must be constructed and compared before point-by-point spectral information is available.

In a combined system it will be necessary to comprise between the 6.7 mrad instantaneous field of the long-wavelength system and the 1-mrad proposed for the short-wavelength system. Changing the instantaneous field of view β will change both the performance of each system and necessitate changes in the spectrometer designs (see eqs. 5, 12, and 16). If we put β = 3 mrad, we find that the sensitivity of the long-wavelength system is reduced about 5 times. This is unfortunate but not as serious as might appear at first sight, for two reasons. First, for objects which subtend the original larger field it will be possible to carry out spatial integration either in the processing or by eye on the strip maps produced. Second, the original specifications were drawn up with due consideration of the very small differences in spectral emissivity anticipated for the lunar surface. For terrestrial applications, larger spectral emissivity differences are expected, and it is unlikely that such small differences will be significant. Thus, the fivefold loss in sensitivity, though unfortunate, is acceptable. Examination of equation 5 shows that the design of the long-wavelength spectrograph is eased when the smaller β is used. It would be practical to use a rock salt prism rather than the very coarse grating recommended for the then larger field system. The threefold increase in instantaneous field for the short-wavelength instrument will, of course, result in poorer ground resolution. However, the ground resolution will still be much finer than can be obtained from the much higher orbital altitudes, so it can still be regarded as satisfactory. The sensitivity will be improved, but the spectrograph concept must be changed to avoid having to use an impractically large prism. Several alternatives are possible. A Fresnel prism (i.e., several prisms used in parallel) could be employed. Alternatively, two grating instruments could be used, each covering part of the wavelength range; but this would necessitate the use of a dichroic beam splitter to separate the wavelength ranges. Probably a more satisfactory solution would be to use a rectangular entrance slit defining a 1 × 3-mrad field. The spectrograph optical system could then be identical to that recommended for the short-wavelength orbital system, except that the detectors and entrance slit would be lengthened 3 times, parallel to the prism axis. If the longer entrance slit

dimension were projected onto the ground at right angles to the scan lines, this system would still be compatible with the 3-mrad long-wavelength system.

In order to facilitate data reduction and handling, it would be desirable to use a common field stop for both systems. This would ensure that all signals at any instant of time relate to identical parts of the object field. Some form of beam splitter would be required to do this with relay optics to a second smaller field stop if nonidentical fields were used, as suggested above.

6.2. SIZE, WEIGHT, AND POWER REQUIREMENTS

Accurate assessments of size and weight of these units is difficult at this stage. In particular, the success of the optical designers in reducing the f-number of the spectrograph optics will play a major part in determining the overall size and weight. The estimates given in table III are based on those for existing scanners. Most of the estimated power requirement stated would be absorbed in the scan-mirror drive system and dissipated in overcoming wind resistance to the rotating scan mirror. This resistance would not be present in an orbital system,

TABLE III. SPECIFICATIONS FOR AIRBORNE MULTISPECTRAL SENSORS

	Short-Wavelength System	Long-Wavelength System	Combined System
Instantaneous field of view	1 × 1 mrad	6.7 × 6.7 mrad	3 × 3 mrad
Collector diameter	15 cm	15 cm	15 cm
Dispersing element	SiO prism	50 lines/mm grating	SiO & NaCl prisms
Wavelength coverage	0.3-2.5 μ	8-14 μ	0.3-2.5 & 8-14 μ
Spectral resolving power	10	25	10 & 25
Angular coverage	$\pm 40^{o}$	$\pm 40^{o}$	$\pm 40^{o}$
Ground resolution from 30,000 ft	30 ft	200 ft	90 ft
Additional wideband channels	4.5-5.5 & 10-12 μ	1.5-1.8 μ	4.5-5.5 μ
Approximate dimensions*	2 × 2 × 4 ft	2 × 2 × 4 ft	2 × 2 × 6 ft
Approximate weight	200 lb	200 lb	300 lb
Approximate power requirements	700 w	700 w	700 w

*Excluding recording and processing systems and cryogenic storage.

which would be operating in vacuum; therefore it is clear that the power requirements for such orbital systems would be much less than those quoted here for the airborne systems.

In the absence of detailed design information on the spectrograph optics, it would be premature to attempt design layouts for the overall systems, though these will be generally similar to the system shown in figure 15.

6.3. DATA PROCESSING

The most reasonable method of storing and transporting the data obtained in the airborne spectrometer experiments is to record all the raw data on magnetic tape. The weight restrictions would be relaxed with an airborne vehicle as contrasted to a present-day satellite system both with respect to bulk of data collected in a single flight and the weight that can be returned to earth. Also, a general-purpose computer can be used for processing the data, so that the requirement for much special-purpose equipment would be unnecessary and several processing schemes could be tried for the same data. This second advantage allows various processing arrangements to be evaluated with realistic data with a maximum of ease and flexibility.

7
CONCLUSIONS

This study has established the feasibility of dispersive multispectral scanning as a remote sensing technique. There are inevitably boundaries to the usefulness of such systems imposed by considerations such as those of cost and the state of the art. One of the most useful results of the study in addition to establishing the feasibility of multispectral sensing is the indication it provides of areas in which more detailed study is required to establish these boundaries with precision. The remainder of this final section of the report covers these areas in turn.

7.1. DESIGN OF THE SPECTROGRAPH OPTICS

As explained in sections 3.1 and 3.2, the size of the combined detector and field lens array is proportional to the f-number of the spectrograph's optical system. Thus the smaller the f-number can be, the smaller the array and therefore the cryostat become. Because the initial and the operating costs of cryostats will increase very rapidly with size, this is a major item in the feasibility of any given system.

7.2. SCANNER APERTURE SIZE

Throughout the report, apertures greater than 6 in. in diameter have not been considered. Experience with monochromatic airborne scanner systems has shown that larger apertures would require an overall instrument size too large to be compatible with airborne or spaceborne operation, particularly in conjunction with other experiments. On the other hand, other things being equal, sensitivity can only be increased or ground resolution improved by increasing the aperture. Thought should therefore be given to the feasibility of using larger systems, particularly for the earth science applications requiring fine ground resolution.

7.3. PREPROCESSING

Although the study shows that various data processing schemes can be implemented to distinguish spectral differences, it is clear that preprocessing cannot be implements sensibly unless firm statistical data on target and background spectra are available. Such data for terrestrial applications are only now being collected in the fields of agriculture and geology. For the limited objective of determining the acidity or basicity of various parts of the lunar surface by use of relatively low resolution spectra in the 8-14-μ band, such a processor could probably be designed on the basis of available laboratory data; but in other cases adequate data do not appear to exist. Further thought should also be given to the possibilities of adaptive processing as a means of solving the data bulk problem.

7.4. REQUIRED SIGNAL-TO-NOISE RATIO

In most monochromatic scanner applications, an S/N of 1 is often assumed to be adequate, but this is satisfactory only when the eye can integrate areas on the strip maps obtained. In the very simple case in which the presence of a shallow absorption band is to be detected in a single spatially resolved element, a channel S/N of at least 5 would be required to give an acceptable detection probability and false alarm rate. This criterion of a S/N of 5 has been used throughout the report. However, it seems clear that in more, or in less, restricted circumstances higher S/N might be required or lower ones suffice, respectively. Generalizations, like those for data processing problems, are difficult; specific cases have to be studied. Nevertheless, there is clearly need for further thought in this area.

7.5. IR DETECTOR PACKAGE

The performance characteristics (D^*) used for Ge:Cu and Ge:Hg detectors throughout this report are typical of current state-of-the-art detectors used under normal operating conditions. Efficient matched preamplifiers suitable for use under operational conditions do not appear to

have been developed. Considerable improvements can be obtained, under limited laboratory conditions, if the ambient photon flux falling onto the detectors is reduced by cold shielding and filtering. Under these conditions, the detector impedance becomes very high. This may well be a more satisfactory way of obtaining increased sensitivity or improved spatial resolution than by increasing the entrance aperture size, and merits study and development.

7.6. OTHER APPROACHES

In compliance with the work statement of this contract, no consideration has been given to the use of techniques other than dispersive, for spectral resolution. Willow Run Laboratories has a good deal of experience with multispectral scanners in which the spectral resolution is carried out by means of optical filters used with an array of detectors placed in the focal plane of the scanner. Such systems have the serious disadvantage that a given ground resolution element beneath the aircraft is scanned sequentially by the various detectors. To compensate for this, appropriate delays must be used in the various data channels. What is worse, unless relatively complicated optical compensation is employed, the lines scanned by the various detectors diverge slightly on either side of the nadir. The use of dispersive techniques is thus very attractive in that all detectors are imaged onto the spectrograph entrance slit and thus not only scan identical paths on the ground but do so in time coincidence. However, as we have seen, the spectrograph optical system will in some circumstances be quite complex. Thus, when specific system requirements are being considered, the detector-array approach should not be dismissed without some study of the relative merits of the two approaches as applied to the particular requirements in question.

Appendix
DERIVATION OF THE PARAMETRIC EQUATIONS

Equations are developed below which describe the performance of a generalized multispectral dispersive scanner in terms of selected system parameters. Because of the relations which exist among many sets of parameters there is no unique way of doing this. However, the final equations are given in terms of a set of independent parameters which are judged to be the most useful in the sense that any one can be varied, at any rate, over some range of feasible values without necessitating changes in any of the other members of the selected set.

A.1. SCANNER GEOMETRY

First we consider a simple telescope (fig. 18) consisting of a square detector in the focal plane and on the axis of a positive lens (or Cassegrainian reflector). A 45^{o} mirror is placed in front of the lens and rotated about an axis parallel to that of the lens. Thus the field of view of the telescope sweeps around a circular path normal to the telescope and scan mirror axis (fig. 19). If this scanner is placed on a vehicle with its rotational axis horizontal, the sweeping field will intercept a strip on the ground. If the field is square (with the sides parallel and perpendicular to the ground track at the nadir) and contains a solid angle of β^2 steradians, the width of this strip will be $\beta H/\cos\alpha$, where H is the vehicle altitude, and α is the angle between the line of sight and the vertical. Thus the strip width minimum is βH directly beneath the vehicle. Further, if the vehicle moves with a velocity V in the direction of the axis, successive scan lines will be moved relative to the previous line by a distance Vt, where t is the time in which the scan mirror makes one revolution. Thus to make the scanned strips contiguous directly beneath the scanner we must have

$$Vt = \beta H \tag{1}$$

If the angular velocity of the scan mirror about its axis is $\dot{\alpha}$, then we have $t = 2\pi/\dot{\alpha}$ and can substitute and rearrange equation 1 to give

$$\dot{\alpha} = \frac{2\pi(V/H)}{\beta}\ \text{rad/sec} = \left(\frac{60V/H}{\beta}\ \text{rpm}\right) \tag{2}$$

Any point on the ground covered by a scan line will be in the field of view for a dwell time τ

$$\tau = \beta/\dot{\alpha}\ \text{sec}$$

$$= \beta^2/2\pi(V/H)\ \text{sec} \tag{3}$$

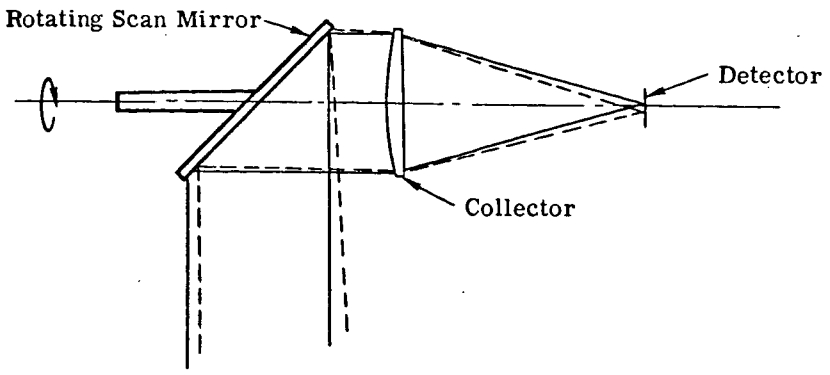

FIGURE 18. SCHEMATIC OF SIMPLE SCANNING SYSTEM

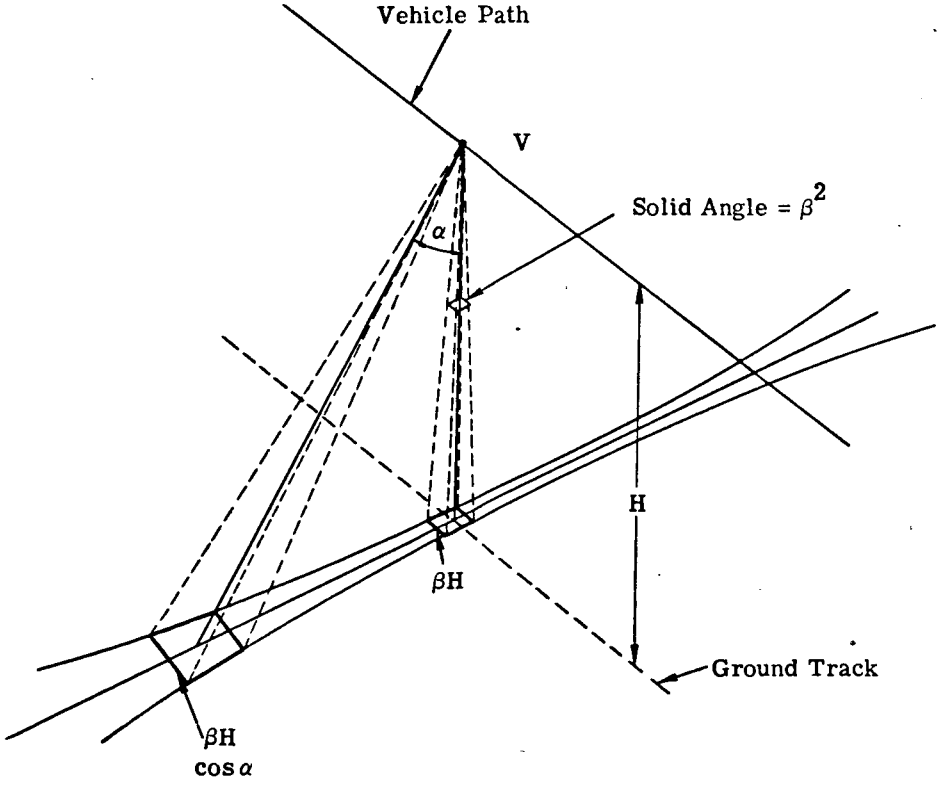

FIGURE 19. SCHEMATIC REPRESENTATION OF SCANNER VIEWING GEOMETRY

In the simple scanner described there will be a "dead time" during the part of each revolution of the scan mirror during which the "beam" of the instrument is not looking in a direction of interest. In general, the direction of interest lies within an angle of 60^{o} to 180^{o} centered on the downward vertical. This dead time can within limits be reduced by various techniques such as the use of a multifaced scanning mirror. This would have the effect of reducing the scan mirror rpm given by equation 2 and increasing the dwell time given by equation 3 by a factor n equal to the number of faces used. Thus we have:

$$\dot{\alpha} = \frac{2\pi(V/H)}{n\beta} \tag{2a}$$

and

$$\tau = \frac{n\beta^2}{2\pi(V/H)} \tag{3a}$$

A.2. THE MATCHING SPECTROGRAPH

Next we consider replacing the single detector in the focal plane of the telescope by a spectrograph whose entrance slit is in the telescope focal plane as shown schematically in figure 20. The D's are the diameters and the F's the focal ratios of the various optical elements. We assume that D_2, D_2', and the aperture of the dispersing element are all equal (in practice the smallest of these elements will act as the effective stop for all of them).

The field of view of the scanner is fixed by the spectrograph entrance aperture d_1, such that if the aperture is square and defines the field of a solid angle of β^2 steradians, then

$$\beta = \frac{d_1}{F_1 D_1} \tag{4}$$

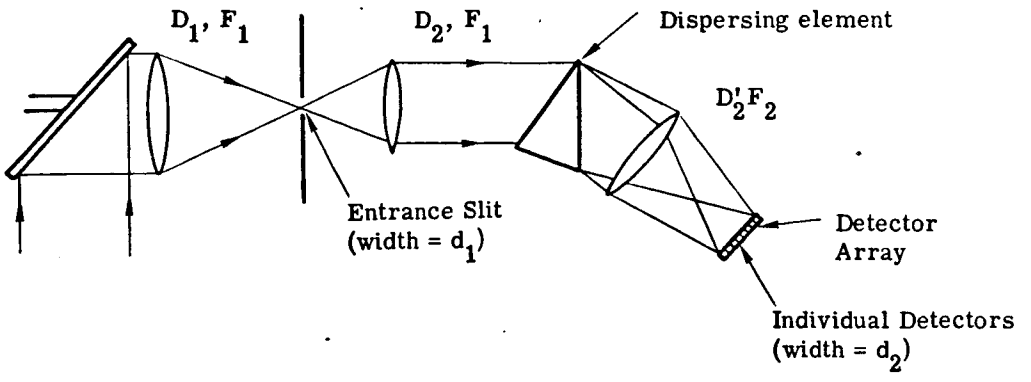

FIGURE 20. SCHEMATIC OF MULTISPECTRAL DISPERSIVE SCANNER

If the angular dispersion of the prism or grating is $d\theta/d\lambda$, then to obtain a resolved wavelength interval of $\delta\lambda$ in the most efficient way the entrance and exit slits must both subtend $\frac{d\theta}{d\lambda}\delta\lambda$. Since also the aperture ratio of the scanner telescope and the entrance optics of the spectrograph must be matched,

$$\frac{d_1}{F_1 D_2} = \frac{d\theta}{d\lambda}\delta\lambda$$

or, substituting for d_1/F_1 in equation (4):

$$\frac{\beta D_1}{D_2} = \frac{d\theta}{d\lambda}\delta\lambda$$

thus,

$$\delta\lambda = \frac{D_1\beta}{D_2(d\theta/d\lambda)} \tag{5}$$

Next, because the individual detectors of the array act as exit slits, the detector size, d_2, is given by

$$\frac{d_2}{D_2 F_2} = \frac{d\theta}{d\lambda}\delta\lambda = \frac{\beta D_1}{D_2}$$

or

$$d_2 = \beta D_1 F_2 \tag{6}$$

The detector can, of course, be made larger to increase the effective $\delta\lambda$, but this would, in general, be less efficient than increasing $\frac{d\theta}{d\lambda}$ by altering the prism apex angle or grating spacing as appropriate, if this is feasible. However, it may be desirable to vary the bandwidth across the spectrum by using exit slits (detector widths) wider than optimum by a factor m, which is at the disposal of the designer and may well vary across the array. Thus the new waveband is m times wider than that given by (5), or

$$\delta\lambda' = \frac{mD_1\beta}{D_2(d\theta/d\lambda)} \tag{5a}$$

and

$$d' = m\beta D_1 F_2 \tag{6a}$$

where d' = the width of the enlarge detector. The detector height will, however, still be given by equation 6. Further, if the detector array is to cover a wavelength range $\Delta\lambda$, then L, the total length of the array, must be equal to the length of a detector as defined by equation 6 multiplied by M, the number of resolved wavelength intervals (as defined in equation 5) contained in $\Delta\lambda$. (Note: $\delta\lambda$ will vary, because $d\theta/d\lambda$ varies with λ; therefore it will not, in general, be correct to put $m = \Delta\lambda/\delta\lambda$.) Thus

$$\begin{aligned} L &= Md_2 \\ &= M\beta D_1 F_2 \end{aligned} \tag{7}$$

We can regard equation 5 as the basis for the design of the spectrograph, using it to choose the size of the prism or grating, D_2, in terms of other parameters. However, because $d\theta/d\lambda$ is, in general, a function of wavelength, some compromise will have to be made in the choice of the wavelength used as a basis for the choice of D_2. Thereafter, the wavelength resolution and sensitivity can be controlled to some extent by increasing individual detector sizes as explained. Equation 5a then gives the wavelength resolution in terms of the other parameters.

A.3. PERFORMANCE CALCULATIONS

Two situations must be distinguished and treated separately. First, we must consider the case in which the noise level is independent of the signal level. The various solid-state infrared detectors will fall in this class. Even those which are radiation noise limited can be treated as belonging to this class because generally the signals can be thought of as small changes in a much larger and essentially constant radiation level. Thus the noise is essentially indepenent of the signal level and the detector can be characterized by a specific detectivity, D^*. The photomultipliers, however, are in a second class. They are shot noise limited, and this noise is proportional to the square root of the cathode photocurrent, which is itself proportional to the incoming radiation level which may vary considerably at the wavelengths at which such detectors are used.

A.4. NOISE INDEPENDENT OF SIGNAL LEVEL

If the detector noise is independent of signal level, it is desirable to make the f-number of the cone of radiation falling onto the detectors as small as possible to optimize the NEP (noise equivalent power). To reduce the aperture ratio below that practical in the design of the spectrograph, an array of square or rectangular field lenses could be used in the focal plane of the spectrograph in place of the detector array (see sec. 3.1). Individual detectors would then be placed in the focal planes of each field lens. All the preceding equations still apply except that

d and d' will now represent the sizes of the field lenses rather than of the detectors and L is the length of the field lens array. It can easily be shown that the optimum size for each detector d'' is then given by replacing d' by d'' and F_2 by the f-number of the individual field lens F_f in equation 6a, which then becomes

$$d'' = m\beta D_1 F_f \tag{6b}$$

The detectors now have the effective area of the prism or grating imaged onto their surfaces; therefore they will in general be squares with sides given by d'' of equation 6b. The field lenses, however, have heights given by equation 6 and widths by equation 6a and so will only be square if m = 1.

The sensitivity of a given detector channel can be computed in the usual way, by writing down the S/N as the ratio of the power falling onto the detector and the NEP of the detector.

Assuming a uniform field of view with spectral radiance N, the power reaching a given detector is:

$$P_\lambda = N_\lambda \, \delta\lambda' \times \frac{\pi D^2}{4} \times \beta^2 \times (\text{o.e.}) \tag{8}$$

where $\delta\lambda'$ is the resolved wavelength defined by equation 5a. We also use the standard formula

$$(\text{NEP})_\lambda = \frac{(\text{Detector area} \times \text{Electronic bandwidth})^{1/2}}{D^*_\lambda \times \text{s.e.}} \tag{9}$$

Here "signal efficiency" takes into account the extent to which the amplifier noise factor and the signal shaping due to the finite amplifier bandwidth degrades the S/N of the system.

We can use equation 6a or 6b, as appropriate, to obtain the detector area in terms of system parameters. It will be seen that we can combine both cases by putting

$$\text{Detector area} = m^p \beta^2 D_1^2 F_d^2 \tag{10}$$

where p = 1 if field lenses are not used, p = 2 if field lenses are used, and F_d is the f-number of the beam at the detector, that is, of the field lens if a field lens is used or of the spectrograph output beam if a field lens is not used.

If the electronic bandpass of the amplifier is chosen to optimize the probability of detecting a point target, then the bandwidth will be given by

$$\Delta f \approx 1/2\tau$$

or if equation 3a is used,

$$\Delta f = \pi(V/H)/\beta^2 n \tag{11}$$

Thus we can write

$$(NEP)_\lambda = \frac{D_1 F\sqrt{\pi m^p (V/H)}}{D^*_\lambda \sqrt{n}\ (s.e.)}$$

Thus from 8 we finally obtain

$$\left(\frac{S}{N}\right)_{I\lambda} = N_\lambda\, \delta\lambda' \frac{1}{4}\sqrt{\frac{\pi n}{m^p}} \cdot \frac{D_1 D^* \beta^2}{F_d \sqrt{V/H}}\ (o.e. \times s.e.) \tag{12}$$

Because $\delta\lambda'$ is related to m by equation 5a, it is sometimes more convenient to rewrite equation 12 in terms of $\delta\lambda$, defined in equation 5 which is independent of m. Then we have

$$\left(\frac{S}{N}\right)_{I\lambda} = \frac{1}{4} N_\lambda \sigma\lambda \sqrt{\frac{\pi n}{m^{p-2}}} \cdot \frac{D_1 D^* \beta^2}{F_d \sqrt{V/H}}\ (o.e. \times s.e.) \tag{12a}$$

However, if this form is used, it must be remembered that the spectral interval actually resolved is not $\delta\lambda$ but $m\,d\lambda$.

Though the detector size and electronics bandwidth have disappeared from these relations, it must always be remembered that equations 10 and 11 are implicit, so that values of parameters which lead to impracticable detector sizes and bandwidths given by equations 10 and 11 must be avoided.

It should also be remembered that effects of path transmission may have to be taken into account, either by including this factor in the overall efficiency or by regarding N_λ as an "apparent radiance." In the signal-to-noise-ratio equations, (12) and (12a), the whole of the radiant power falling on each detector is regarded as being "signal." However, more often the signal in which we shall be interested will be a differential due to a small change in the temperature, emissivity, or reflectivity from one elementary field (resolution element) to the next. Equations 12 and 12a can readily be put into differential form by replacing N_λ by ΔN, $\Delta\epsilon N_\lambda$, $\int_{T_1}^{T_2} \frac{\partial N_\lambda}{\partial T} dT$, or whatever term is appropriate.

A.4. SHOT-NOISE-LIMITED DETECTORS

For a shot-noise-limited detector, such as a photomultiplier, the equivalent noise current at the photocathode is given by the well-known formula

$$I_N = k\sqrt{2ei\Delta f} \tag{13}$$

where e = the electronic charge

i = the total photocathode current

Δf = the noise bandwidth

k = the noise factor of the multiplication process as in a photomultiplier tube

The corresponding signal current is

$$I_S = P_\lambda R_c \times (\text{s.e.})$$

where P_λ = the effective spectral radiant power impinging on the photocathode, in watts, and R_c = the photocathode radiant sensitivity, in amperes per watt. Thus

$$\frac{S}{N} = \frac{P_\lambda R_c}{k\sqrt{2ei\Delta f}} \times (\text{s.e.}) \tag{14}$$

Now

$$i = I_S + I_D$$

where I_D = the dark current; but in practice except at very low light levels we can write $I_D \ll I_S$, so that $i = I_S = P_\lambda R_c$ and

$$\left(\frac{S}{N}\right)_\lambda = \frac{1}{k}\sqrt{\frac{P_\lambda R_c}{2e\Delta f}} \times (\text{s.e.})$$

Using equation 8 for P_λ and equation 11 for Δf, we obtain

$$\left(\frac{S}{N}\right) = \frac{\beta^2 D_1}{2k}\sqrt{\frac{nR_c N_\lambda \delta\lambda\ (\text{o.e.})}{2e(V/H)}} \times (\text{s.e.})$$

$$= 4.2\beta^2 \times 10^8 D_1 \sqrt{\pi n R_c N_\lambda \delta\lambda (\text{o.e.})/(V/H)} \times (\text{s.e.}) \tag{15}$$

putting $k = 1.2$ and $e = 1.6 \times 10^{-19}$ coulomb.

As before, path transmission should be included in the optical efficiency, or alternatively N_λ should be regarded as the apparent radiance as measured at the instrument.

A.5. DIFFERENTIAL SIGNALS WITH SHOT-NOISE-LIMITED DETECTORS

At the wavelengths at which shot-noise-limited detectors can be used in orbital surveying experiments, the sun is the only significant illuminating source. Thus if H_λ is the solar spectral irradiance at the target we can put

$$N_\lambda = \frac{1}{\pi}\rho_\lambda H_\lambda \cos\alpha$$

where ρ_λ is the appropriate reflection coefficient for the directions of illumination and observation, both having two components: azimuth and elevation. Now because H_λ and the angle of illumination will be constant over a period of several scans, we can put

$$N_\lambda = \frac{1}{\pi}\rho_\lambda H_\lambda$$

and

$$\Delta N_\lambda = \frac{1}{\pi}\Delta\rho_\lambda H_\lambda$$

Substituting in equation 8 we find

$$P_\lambda = \frac{1}{\pi}\rho_\lambda H_\lambda \delta\lambda \frac{\pi}{4} D_1^2 \beta^2 \text{ (o.e.)}$$

and

$$\Delta P_\lambda = \frac{1}{\pi}\Delta\rho_\lambda H_\lambda \frac{\pi}{4} D_1^2 \beta^2 \text{ (o.e.)}$$

so that

$$i = P_\lambda R_c$$

$$= \rho_\lambda H_\lambda \delta\lambda R_c \frac{1}{4} D_1^2 \beta^2 \text{ (o.e.)}$$

Then substituting in equation 14, in which we first replace P_λ by ΔP_λ, and using equation 11 for Δf, we obtain

$$\left(\frac{S}{N}\right)_{S\lambda} = 4.2 \times 10^8 D_1 \beta^2 \Delta\rho_\lambda \sqrt{\frac{nR_c H_\lambda \delta\lambda(\text{o.e.})}{\rho_\lambda (V/H)}} \times \text{(s.e.)} \qquad (16)$$

REFERENCES

1. J. I. Trombka, Least-Squares Analysis of Gamma Ray Pulse Height Spectra, Tech. Report 32-373, California Institute of Technology, Jet Propulsion Laboratory, Pasadena, Calif., December 15, 1962.
2. E. Franzgrate et al., "Chemical Analysis of Surfaces Using Alpha Particles," J. Geophys. Res., Vol. 70, March 1965, pp. 1311-1327.
3. R. J. P. Lyon, "Infrared Spectral Analysis of the Lunar Surface from an Orbiting Spacecraft," Proc. Second Symposium on Remote Sensing of Environment, Report No. 4864-2-X, Institute of Science and Technology, The University of Michigan, Ann Arbor, October 1962, p. 309.
4. J. Conel, private communication.
5. W. A. Hovis, Jr., and W. R. Callahan, Infrared Reflectance Spectra of Igneous Rocks, Tuffs, and Red Sandstone from .5-25 μ, Goddard Space Flight Center, Greenbelt, Maryland, unpublished paper, 1965.
6. R. J. P. Lyon and E. A. Burns, Feasibility of Remote Compositional Mapping of the Lunar Surface, NASA 49(04), Stanford Research Institute, Menlo Park, California, 1963, p. 8.
7. R. J. P. Lyon, Evaluation of Infrared Spectrophotometry for Compositional Analysis of Lunar and Planetary Soils, NASA 49(04), Stanford Research Institute, Menlo Park, Calif., 1963, p. 100.
8. S. J. Gawarecki, R. J. P. Lyon, and W. Nordberg, "Infrared Spectral Returns and Imagery of the Earth from Space and Their Applications to Geologic Problems," Proc. Third Goddard Memorial Symposium, Am. Astronaut. Soc. 1965 (in press)
9. I. Sattinger and F. Polcyn, Applications of Earth-Observation Spacecraft; Vol. I: Benefits and Manned Earth Orbital Experiments, Report No. 7219-1-F(I), Willow Run Laboratories, Institute of Science and Technology, The University of Michigan, Ann Arbor, February 1966.

RELATED REPORTS

COMPARATIVE MULTISPECTRAL SENSING, M. R. Holter and F. C. Polcyn, Rept. 2900-484-R, Institute of Science and Technology, The University of Michigan, Ann Arbor, June 1965 (CONFIDENTIAL).

DIURNAL AND SEASONAL VARIATIONS IN RADIATION OF OBJECTS AND BACKGROUNDS, 4.5-5.5-μ SPECTRAL REGION, L. D. Miller and R. Horvath, Rept. 6400-32-T, Institute of Science and Technology, The University of Michigan, Ann Arbor, June 1965 (CONFIDENTIAL).

THE INVESTIGATION OF A METHOD FOR REMOTE DETECTION AND ANALYSIS OF LIFE ON A PLANET, M. R. Holter, D. S. Lowe, and R. J. Shay, Rept. 6590-1-P, Institute of Science and Technology, The University of Michigan, Ann Arbor, November 1964 (UNCLASSIFIED).

SPECTRUM MATCHING, R. E. Hamilton, Rept. 6400-18-T, Institute of Science and Technology, The University of Michigan, Ann Arbor, June 1965 (CONFIDENTIAL).

TARGET SIGNATURE STUDY; INTERIM REPORT, VOLUME I: SURVEY, Richard R. Legault and Thomas Limperis, Rept. 5698-22-T(I), Institute of Science and Technology, The University of Michigan, Ann Arbor, October 1964 (CONFIDENTIAL).

TARGET SIGNATURE STUDY; INTERIM REPORT, VOLUME II: RECOMMENDATIONS, Richard R. Legault and Thomas Limperis, Rept. 5698-22-T(II), Institute of Science and Technology, The University of Michigan, Ann Arbor, October 1964 (CONFIDENTIAL).

TARGET SIGNATURE STUDY; INTERIM REPORT, VOLUME III: POLARIZATION Richard R. Legault and Thomas Limperis, Rept. 5698-22-T(III), Institute of Science and Technology, The University of Michigan, Ann Arbor, October 1964 (CONFIDENTIAL).

TARGET SIGNATURE STUDY; INTERIM REPORT, VOLUME IV: BIBLIOGRAPHY (Acoustic, Ultraviolet, Visible, Infrared, and Radar), Thomas Limperis and Raymond S. Gould, Rept. 5698-22-T(IV), Institute of Science and Technology, The University of Michigan, Ann Arbor, October 1964 (SECRET).

TARGET SIGNATURE STUDY; INTERIM REPORT, VOLUME V: CATALOG OF SPECTRAL REFERENCE DATA, Richard R. Legault, Raymond S. Gould, and Thomas Limperis, Rept. 5698-22-T(V), Institute of Science and Technology, The University of Michigan, Ann Arbor, October 1964 (UNCLASSIFIED).

THE INVESTIGATION OF A METHOD FOR REMOTE DETECTION AND ANALYSIS OF LIFE ON A PLANET, Lee D. Miller, 6590-4-F, Willow Run Laboratories, Institute of Science and Technology, The University of Michigan, Ann Arbor, November 1965 (UNCLASSIFIED).

DISTRIBUTION LIST

NASA Headquarters, D.C.	Copies
Miss Winnie Morgan, Technical Reports Officer	2
Dr. Peter C. Badgley, Program Chief	3
Theodore A. George	1
Richard J. Allenby	1
NASA/MSC-Houston	
Leo F. Childs, Chairman, Aircraft Coordination	1
Ed. Zeitler, Data Center	20
Authors	10

USGS/Washington	Copies
William T. Pecora	1
Research Coordinator	2
Remote Sensing Evaluation and Coordination Staff (RESECS)	2
Chief Geologist	1
Associate Chief Geologist	1
Assistant Chief Geologists (4)	4
Chief Hydrologist	1
Chief Topographic Engineer	1
Discipline Coordinators (4)	4
Bernardo Grossling	1
William Hemphill	1
Allen Heyl	1
Robert Moxham	1
Alan Kover	1
David Southwick	1
Isidore Zietz	1
Stephen J. Gawarecki	1
Librarian	1

USGS/Menlo Park	
Ernest H. Lathram	1
Hal T. Morris	1
Robert E. Wallace	1
Edward W. Wolfe	1
George Gryc	1
Max Crittenden	1
Parke Snavely, Jr.	1
Arthur Grantz	1
Librarian	1

USGS/Denver	
Arthur B. Campbell	1
Robert L. Christiansen	1
David F. Davidson	1
Ross B. Johnson	1
Daniel R. Shawe	1
Robert H. Morris	1
Tom Hendricks	1
Librarian	1

USGS/Flagstaff	
Librarian	1
Gerald S. Schaber	1

US Dept. of Agriculture	
A.B. Park	1

US Air Force	
J.F. Cronin (AFCRL)	1

US Navy	
A.G. Alexiou (NAVOCEANO)	1

Other Cooperating Investigators	Copies
R.N. Colwell, Univ. Calif	1
J. Lintz, Univ. Nevada (Houston)	1
R.J.P. Lyon, Stanford Univ.	1
D.B. Simonett, Univ. Kansas	1
E.H.T. Whitten, Northwestern Univ.	1
William Vest, IITRI, D.C.	1
NAS/NRC Advisory Comm. Chm.	1
R.W. Peplies, E. Tenn. State Univ.	1